2003

Investigation into the use of a tapered element oscillating microbalance for real-time particulate measurement

Marcus Gilbert
West Virginia University

Investigation into the Use of a Tapered Element Oscillating Microbalance for Real-Time Particulate Measurement

by

Marcus Gilbert

THESIS

Submitted to the College of Engineering and Mineral Resources
at
West Virginia University

in partial fulfillment of the requirements for the degree of

Master of Science
in
Mechanical Engineering

Nigel N. Clark, Ph.D., Chair
Christopher M. Atkinson, Sc.D.
Gregory Thompson, Ph.D.
Ralph D. Nine, MSME

Department of Mechanical and Aerospace Engineering

Morgantown, West Virginia
2002

Abstract

Investigation into the Use of a Tapered Element Oscillating Microbalance for Real-Time Particulate Measurement

Marcus S. Gilbert

Characterizing particulate matter (PM) in diesel exhaust emissions during transient test cycles has been a challenge for researchers. Acquisition of real-time PM data was proposed by the use of a Rupprecht and Patashnick Co., Inc. Series 1105 Diesel Particulate Monitor Tapered Element Oscillating Microbalance (TEOM) mass measuring device. The objectives of testing with a TEOM diesel particulate analyzer were to validate its collection capability and evaluate its real-time characteristics on transient test cycles. Conventional PM filtration was used as the base line for evaluating the TEOM collection capability. To evaluate real-time TEOM characteristics, the real-time mass rate data were separated into positive and negative values, then integrated over the duration of the test. The integrated positive mass was divided by the integrated negative mass to create a positive-to-negative mass ratio. This ratio was indicative of real PM collected versus moisture released from the filter. TEOM sample tube temperatures at 35°C yielded the best TEOM to conventional PM filtration ratio. However, a compromise between conventional filter data and real-time data was made in selecting the temperature set point of 40°C as the most desirable sampling temperature. Sample flow rate was varied from one to four liters per minute (lpm). The 1 lpm set point provided the best TEOM to conventional filtration ratio. The flow rate of 3 lpm was chosen to be a compromise between TEOM to conventional filtration ratio and real-time results. The best TEOM to conventional filtration ratio measured was 0.97. The filter collection efficiency of a new filter was found to be a significant source of variability. When the initial test with a new filter was disregarded, the 99% confidence interval in TEOM results was ±4.3%. In comparison, the 99% confidence interval in conventional PM results was ±1.7%.

Acknowledgements

The author thanks Nigel Clark, Chris Atkinson, Greg Thompson (for the advice and direction I should have listened to), and Ralph Nine for their support, guidance, and motivation. All of this has played an important role in helping understand the depth and diversity of the words “research” and teamwork. I would also like to thank Richard Atkinson, Mike Traver, Wayne Hildebrand, Tom Spencer, and Tom McDaniel for always helping me without complaint. I would still be lost if it were not for their expertise. I would like to thank Matt Hawkins and Steph Paree (now Hawkins): their garage provided a perfect haven for a “gear head” like me, and the friendship that provided the brotherhood that everyone deserves. I would like to thank Steve Hamm, Jim Daley, and Bill Marty for being good friends to keep. Jim even more for being the Jim Daley more people should know, himself. Life becomes simpler after you meet him, an important thing to embrace. I hope he remembers. I would like to thank Jen Hoppie for talking me into graduate school and helping me find the path in life I knew was right, but was not aware of. A special thank you to Georgian Steinhardt, I deeply appreciate the sacrifices you have made to help me through this. I know having a “little boy” around the house was difficult. I want to thank my loving parents, Steve and Charlotte. I love the both of you with all my heart. I would not have made it very far in life if it were not for your love and support. I owe all I have to you. Alison, only you could even begin to understand my thanks, because you are the only one that ever could. Thank you for taking care of me throughout the writing of this. You have enlightened my life by giving it cause and meaning. Most importantly, you make me feel good about myself. I hope I can return those favors some where down our road together.

Table of Contents

List of figures

List of Tables

Nomenclature

Abbreviations and Symbols

CBD	Central Business District
CFR	Code of Federal Regulations
CO	Carbon Monoxide
CO_2	Carbon Dioxide
COV	Coefficient of Variance
DI	Direct Injection
EERL	Engine and Emission Research Laboratory
EPA	Environmental Protection Agency
FTP	Federal Test Procedure
HC	Hydrocarbon
HP	Horsepower
I/O	Input and Output
IDI	Indirect Injection
ISF	Insoluble Fraction
LED	Light Emitting Diode
MC	Mass Concentration
MHz	Megahertz
NO_x	Oxides of Nitrogen
PC	Personal Computer
PM	Particulate Matter
PPM	Parts Per Million
PTFE	Polytetrafluoroethylene
R&P	Rupprecht & Patashnick
RH	Relative Humidity
s_x	The standard deviation of the data set "x"
s_y	The standard deviation of the data set "y"
SOF	Soluble Organic Fraction
T90	90 percent boiling point temperature
TE	Tapered Element
TEOM	Tapered Element Oscillating Microbalance
TFE	Tetrafluoroethylene
THDVETL	Transportable Heavy Duty Vehicle and Emissions Testing Laboratory

TTL	Transistor to Transistor Logic
VOC	Volatile Organic Compound
VW	Volkswagen
WVU FTP 75	West Virginia University engine dynamometer simulation of the Federal Test Procedure 75
$\mathbf{x}$	Data set "x"
$\bar{\mathbf{x}}$	Mean of data set "x"
$\mathbf{y}$	Data set "y"
$\bar{\mathbf{y}}$	Mean of data set "y"

1 Introduction and Objective

1.1 Introduction

In view of increasingly stringent fuel economy standards, diesel engines appear to be attractive alternative powerplants for passenger vehicles. However, despite its inherent efficiency benefit, the diesel engine generally presents a challenging particulate matter (PM) emission control problem. PM is an Environmental Protection Agency (EPA) regulated emission that has attracted special attention due to the investigation of adverse health effects from particulate with aerodynamic diameters of 10μm (PM_{10}) and 2.5μm ($PM_{2.5}$) [1]. Knowing the effect of transient engine changes, for example fueling, injection timing, torque, and speed, on PM in real time could be the key to reduction of PM. Therefore, an instrument is needed to measure real time PM in diesel exhaust.

A Tapered Element Oscillating Microbalance (TEOM) diesel particulate analyzer infers the weight of PM deposited on a small filter in real-time. This is potentially the most feasible method to measure PM emissions in real-time. The TEOM uses a hollow, tapered, cantilever element, which is forced to oscillate at its natural frequency via magnetic field plates and a closed loop control system. The filter is mounted on the free end of the cantilevered tapered element. An internal volumetric flow controller regulates a constant sample of diluted exhaust gas pulled across the filter and through the tapered element. Simplistically, the element and filter system can be represented by a spring-mass system, where a change in mass correlates to a change in the natural frequency. As the filter weight changes due to PM accumulation, the frequency of the element's oscillation changes. This change in frequency is proportional to mass change by the equation below:

$$\Delta M_n = K_o\left(\frac{1}{f_n^2} - \frac{1}{f_{n-1}^2}\right)$$

where ΔM_n is the change in mass in grams, K_o is the TEOM calibration constant, and f_n and f_{n-1} are tapered element (TE) frequency measurements. Unfortunately, the TEOM is sensitive to external vibrations, temperature and pressure variations, and TEOM filter collection efficiency. Filter efficiency changes during collection due to PM accumulation on the filter face and the consequent shrinking of effective pore size. In this research, the use of the TEOM to measure PM is investigated.

1.2 Objective

The objective of this research was to evaluate the use of the TEOM by comparing test results with the conventional gravimetric method. In order to meet these objectives, the following evaluations were performed: (1) TEOM response as (a) instrument temperature, (b) flow, (c) filter media and (d) sample location were changed, (2) filter preconditioning on sampling delay when changing the TEOM filter, (3) real-time TEOM characteristics by comparing its output to real-time gaseous engine emissions.

2 Literature Review

2.1 Particulate Matter Emissions

Particulate emissions created by diesel engines are broken up into two components, the soluble organic fraction (SOF) and the insoluble fraction (ISF). The SOF, or extractable fraction, can be separated from the collected particulate with solvents such as dichloromethane or a benzene–ethanol mixture. When diluted, cooled PM passes through a sampling filter, the soot, other particles, and condensable compounds will be trapped by the filter media and particulate collected on the filter. These trapped HC and oxidation products collected on the filter are labeled the SOF after extraction from the filter [3]. The EPA has set an upper limit on the temperature of PM sampling from diluted engine exhaust of 52°C [2]. It is assumed that this would be the point at which an "acceptable" fraction of condensable hydrocarbon (HC) would stay in the gaseous form to be accounted for by the HC analyzer. The magnitude of SOF in the total particulate ranges from 10 to 90 percent mass, but generally is observed to be around 15 to 30 percent mass [4]. SOF is mainly composed of heavy hydrocarbons that have condensed and grown onto PM particles as the exhaust gas has cooled due to the dilution and mixing with the ambient air. The extractable fraction is one cause for alarm of health concerns and environmental hazards [1,4,5]. This fraction corresponds to 25 to 50 percent of gaseous HC. The exact portion of the total PM depends on operating conditions and engine due to their effect on the distribution of the boiling range of the gaseous HC [5]. The 90% boiling temperature (T90) of the fuel is strongly related to PM production. A high T90 relates to more high temperature boiling point hydrocarbons that tend to be SOF or particulate [3]. The EPA's temperature limit would have to account for a range of possible fuels and engines, implying a question as to its viability for modern alternative fuels. The fuel sulfur content is a strong cause of inorganic content. A linear relationship has been found between the sulfate content in PM to the sulfur content in diesel fuel. However, only 1 to 2 percent of fuel sulfur is generally found in PM [5].

PM in diesel engines is caused by incomplete combustion (oxidation) and pyrolysis of fuel and engine oil. Incomplete combustion is mainly caused in areas of rich equivalence ratios within the cylinder. The central axis of the fuel injection spray pattern is a critical area of PM formation. As the fuel is injected into the cylinder, it has to mix with the existing hot gases. Heywood [4] postulates this creates an inhomogeneous fuel-air mixture, which contains regions that are too lean or too rich to ignite. As soon as cylinder pressure and temperature are high enough, the combustible regions are first to ignite. The fuel and air continue to mix as the flame propagates throughout the cylinder. Some regions that were once too rich or lean to combust now have mixed with air and the increased pressure and temperature cause combustion to continue. Rich areas that do not mix with enough air during this

crucially short time cause the origins of PM. The increased heat and pressure during combustion lead to pyrolysis, or non-oxidation reactions of fuel and engine oil [4]. Another source of PM is from wall quenching, or cooling of combustion gases close to the cylinder and cylinder head walls. Kato et al. [6] found that both SOF and ISF were influenced by wall quenching effects.

2.2 Particulate Filters

For analysis, PM is conventionally captured by sampling a diluted exhaust stream across filter media. Two popular PM filter materials, Pallflex TX40 and T60A20, are similar in material and construction. However, the filters differ in initial collection efficiency, or initial collection rate. Both filters are made from Polytetrafluoroethylene (PTFE) coated glass fibers, and are used in both conventional and TEOM PM collection. Shore [7] states that the T60A20 has a diesel PM collection efficiency of 80% until the "filter has an appreciable coating of particles" after a couple of tests. Furthermore, it is stated that the TX40 has a diesel PM collection efficiency of 98% under all conditions. It is assumed that the diesel collection efficiency of any PM filter would be different for each engine, fuel, and test type due to ISF and SOF variations. Okrent [8] reports that at 0.3 microns, the TX40 filter is 97% efficient and the T60A20 filter is 95% efficient. However, Shore's results show that the TX40 filter produced larger differences between conventional PM and TEOM measurement results than the T60A20. Okrent stated the degree of filter loading did not influence TEOM TX40 collection efficiency [8].

2.3 Tapered Element Oscillating Microbalance

Whitby et al. [9], in 1982, were the first to test an exciting new prototype instrument that allowed real time particulate measurement which truly measured particulate mass without using optical methods. The prototype Tapered Element Oscillating Microbalance, manufactured by Rupprecht and Patashnick Company under the commission of Cummins Engine Company, was tested at the New York State Department of Environmental Conservation facilities for light duty diesel testing. The heart of the instrument was similar to the current generation TEOM unit, a tapered element (TE) firmly mounted at the wide end and with a replaceable filter at the free narrow end. The TE was mounted between two field plates to induce and control oscillation. Measuring the TE frequency of oscillation was an LED and phototransistor system that outputs an AC signal. The signal was amplified and used as a feedback via a conductive path on the TE, which interrupts the field generated by the plates. The amplified signal was also used to analyze the frequency of the TE by means of a counter and then converted to a mass value via a microprocessor algorithm. A sample of diluted exhaust gas was pulled through the filter and tube system, collecting particulate on the filter face. As the mass of the filter changed, so did the frequency of the TE.

The exhaust specimen for the prototype TEOM unit was sampled from a dilution device into an unheated, stainless steel tube, 9.5-mm outside diameter and 50 cm in length. The data were acquired using a Ballston Inc., type CH filter and flow rate of 2.5 liters per minute. The internal temperatures were set at room conditions to create an equivalent environment to the conventional particulate collection method in use. The frequency data output from the TEOM was subjected to a 15 second moving window least-squares linear regression. To compare the TEOM accumulated mass with the conventional method; the conventional filters were weighed immediately after use instead of after the recommended environmental conditioning period. The test bed was a Volkswagen Rabbit Diesel and an Oldsmobile 5.7 L Diesel. These cars ran a combined total of 29 tests cycles consisting of "505 hot starts" (bag III) of the light duty Federal Test Procedure and the New York City Cycle. The results from their tests were an average TEOM over conventional ratio of 0.94 with a coefficient of variance of 13%. It should be noted that these diesels would be considered very dirty by today's standards. The higher PM concentrations from these vehicles could have caused an increase in the collection efficiency of the TEOM filter. The authors noted a negative trend in the mass rate data that followed each positive spike of mass collection. It was proposed that the positive data represented volatile organic compounds (VOC), moisture, and particulate collecting on the filter. During light loading conditions, such as idle or no-load conditions, the VOC and moisture that had built up during heavy loading continued to evaporate from the filter. This exodus of mass from the filter displayed in the data as a negative mass change.

In 1985, Whitby et al. [10] authored another paper geared toward furthering validation of the TEOM as an accepted diesel particulate measurement system. For this testing, only Pallflex T60A20 filters were used instead of Ballston Type CH media. A total of 82 mass comparison tests were performed on a 1979 VW Rabbit Diesel at idle. The Rabbit was used because its emission characteristics had been proven consistent at idle. However, a very high soluble fraction could be expected at idle conditions. The exhaust emissions were diluted through an 18 inch diameter dilution tunnel and sampled through a probe adjacent to the conventional collection method probe. The new TEOM filters, as illustrated in Figure 1, are of the same construction as filters used in this research.

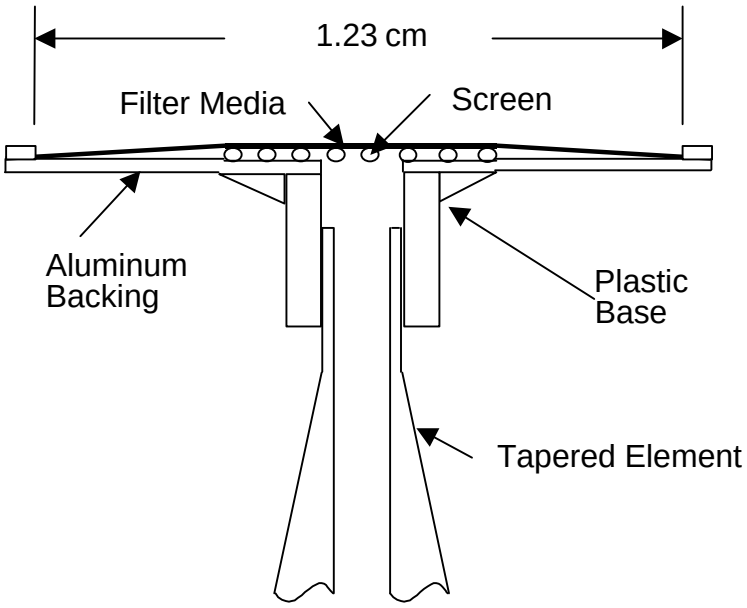

Figure 1: A cut away illustration of the TEOM filter and its mounting on the TE.

EPA guidelines for surface area specific filter flow rate are 0.792-2.638 $l/min/cm^2$. Filter flow rates for the TEOM operation at the low end of EPA guidelines compared to high-end operation did not significantly alter results. Samples for Whitby's research were collected at ranges from 3.2 lpm to 1.1 lpm. To verify the TEOM as an accurate measuring device, 33 non-volatile masses were measured with the TEOM and gravimetrically. Correlation between the two measurements yielded a "virtual 1:1" ratio. Comparison between conventional style particulate collection and TEOM measurements over 27 tests with near equivalent temperatures resulted in a 23% under-collection from the TEOM. The TEOM results were suggested to be lower due to the premise that the amount of volatile species collected on the TEOM filter was lower because of relatively higher vacuum downstream of the filter. Whitby proposed that equivalent masses could be achieved by sampling the TEOM at a lower temperature than conventional filtration. TEOM filters were also tested in a conventional style collection module and gravimetrically weighed. This also resulted in an under-collection (0.85) when compared to conventional methods. Expanding on this idea, TEOM results were compared to the conventional style gravimetric collection on TEOM filters mentioned above, resulting in a ratio of 0.916.

Shore et al. [7] used an undisclosed TEOM model applied to a light duty IDI diesel on the LA4, Japanese 10-mode and European ECE-15 Cycles, as well as a heavy-duty DI diesel on the Federal Test Procedure (FTP). The exhaust sample was drawn from the dilution tunnel adjacent to the conventional PM sample location. From the dilution tunnel, the sample was conveyed through a PTFE tube of similar length to the conventional PM collection system. The external sample tube and TE

housing temperature were set at 50°C. The filter medium used was Pallflex T60A20. The sample flow rate of 1.2 liters per minute was chosen. However, the authors state that flow rates between 0.8 and 3.0 liters per minute produced a proportional mass accumulation. The conclusion reached was that choice of flow rate was not critical.

Thermogravimetric analysis of the filters showed that the amount of volatile material from tests of two different vehicles was similar; however, the TEOM signal from one vehicle exhibited more negative valleys than the other. This suggests that other factors were involved in the negative mass rate trend than the amount of volatiles. The user could not alter the temperatures of the TEOM sample lines and TE housing. Tests where the conventional PM filter temperatures were close to the TEOM filter temperature yielded a better correlation. It was proposed that this phenomena was caused by a greater amount of hydrocarbons being absorbed due to the lower temperatures of the conventional PM filter. The results from the tests yielded TEOM values within 5% to 20 % of conventional PM measurements.

Saito et al. [11] performed a comparison of a TEOM, a high-sensitivity light extinction opacimeter and conventional PM filters. The TEOM sampled from location adjacent to the conventional PM collection point. Filter temperature was held at 50° C and sample flow rate was set to 3 liters per minute during the duration of the testing. The test rig was a 3.4-liter DI diesel powered truck on a chassis dynamometer. As with Shore, Saito found that the TEOM collected mass was lower than the conventional PM method, reporting a 40% TEOM undershoot. Higher TEOM filter temperatures were theorized to be the cause of the large difference with Saito's data: he stated that SOF and moisture was evaporating from the PM. The cooler conventional PM filter was allowing these constituents to remain condensed onto absorbed PM. Also proposed, the moisture and SOF loss caused a slow negative drifting trend in the data.

Okrent [8] investigated the use and optimization of the third generation TEOM. The 1105 model TEOM diesel particulate monitor manufactured by Rupprecht and Patashnick Co. replaced the 1100 series monitor in 1997. Effects of sampling temperatures, sampling rate, filter pressure drop, and filter conditioning were investigated to optimize data quality. The variable that affected the data quality most was sampling temperature. It was found that the temperature did not affect the total mass collected on the filter, but did effect the negative mass trend. By comparing a test run at 35°C and 55°C, it was shown that the amount of negative mass displayed in the data were less in the test sampled at the higher temperature. Okrent proposed that more VOC were collecting on the filter at lower temperatures. Sampling rate was varied from 2 liters per minute to 5 liters per minute, test results concluded that there is no correlation between TEOM and conventional PM filter values as sampling rate was changed. Furthermore, the high filter face velocities caused by sampling at these rates across a

small filter area caused no visual stripping of VOC or water from the filter face. Pressure drop across the filter due to particulate build up was allowed to reach a maximum of 18 inches of mercury and, after this point in loading, flow rate was beginning to be sacrificed. These tests were designed to measure the VOC and water desorption rate. Okrent expected the desorption rate to increase due to the high pressure drop, causing the baseline drift observed by Saito. However, this trend was not observed. Okrent stated that the results were similar at other sampling locations also. Filter conditioning time, or time given for the filter to stabilize in the TEOM unit, was found to be a minimum of 500 seconds.

All of the covered literature compared TEOM results to conventional PM style collection. This method of collection is thought to be reliable because of its acceptance by the EPA. However, a committee correspondence from the Engine Manufacturers Association suggests that laboratory to laboratory variations are significant [12]. A round robin engine test was implemented where three labs tested the same engine to compare results. Lab to lab variations of work specific PM (g/bhp-hr) yielded a coefficient of variation for the hot start FTP test of 17%. The internal coefficient of variation for each lab was reported to be 5%. The TEOM collects mass by the same mechanism and may be susceptible to the same outcome. This could explain at least part of the wide range of TEOM results reported in the literature.

Within the year of 2001, R&P released a new filer cartridge. The new design utilizes a thermo-set plastic carrier to replace the plastic base and aluminum backing, as shown in figure 1. The new design does not utilize a screen under the filter. The functionality of the screen is incorporated into the plastic carrier by molded ridges under the filter. The ridges are directed radially from the center of the filter. The filter material is TX40 and the amount of exposed material is dimensionally the same between the new and old filter. For this study, time limitations hindered testing with this new filter design. Using the new filter, other research at West Virginia University [13] has reported improved initial collection efficiency and correlation with the conventional filter method.

3 Experimental Setup

3.1 Engines and Testing Equipment

The experiments for this research were conducted at two laboratories: the West Virginia University Mechanical and Aerospace Engineering Department Engine and Emissions Research Laboratory (EERL) and the West Virginia University Mechanical and Aerospace Engineering Department Transportable Heavy Duty Vehicle Emissions Testing Laboratory (THDVETL).

3.1.1 Engine and Emissions Research Laboratory

3.1.1.1 Engines and Engine Dynamometer

Two engines were used, a Cummins ISM 370 ESP and a Navistar T444E. Both engines are after cooled direct injection compression ignition engines using 3 parts per million (PPM) sulfur level fuel. The Cummins was an inline 6 cylinder configuration, while the Navistar was a V8 configuration. Engine details are outlined in table 1.

Table 1: Information detailing the specifications of each engine used at the EERL for this testing.

Manufacturer	Cummins	Navistar International
Model	1999 ISM 370 ESP	1999 T444E HT BH210
Displacement	10.8 Liter	7.3 Liter
Advertised Horsepower	370 Hp at 2100 RPM	210 Hp at 2300 RPM
Fuel	3 PPM Sulfur D2	3 PPM Sulfur D2

A General Electric DC dynamometer system was used to load and control the speed of the engines. An IBM-based personal computer (PC) was used to control the dynamometer, using control logic that holds engine speed, while using the fueling rate to match the torque set point. The engine speed and load points came from the Federal Test Procedure (FTP) [2] and an in-house simulation of the light duty chassis FTP 75 (WVU FTP 75) test cycles, illustrated in figures 2 and 3 respectfully. No steady state testing was addressed in this study. It was the focus of this research to evaluate the TEOM applied to transient test cycles.

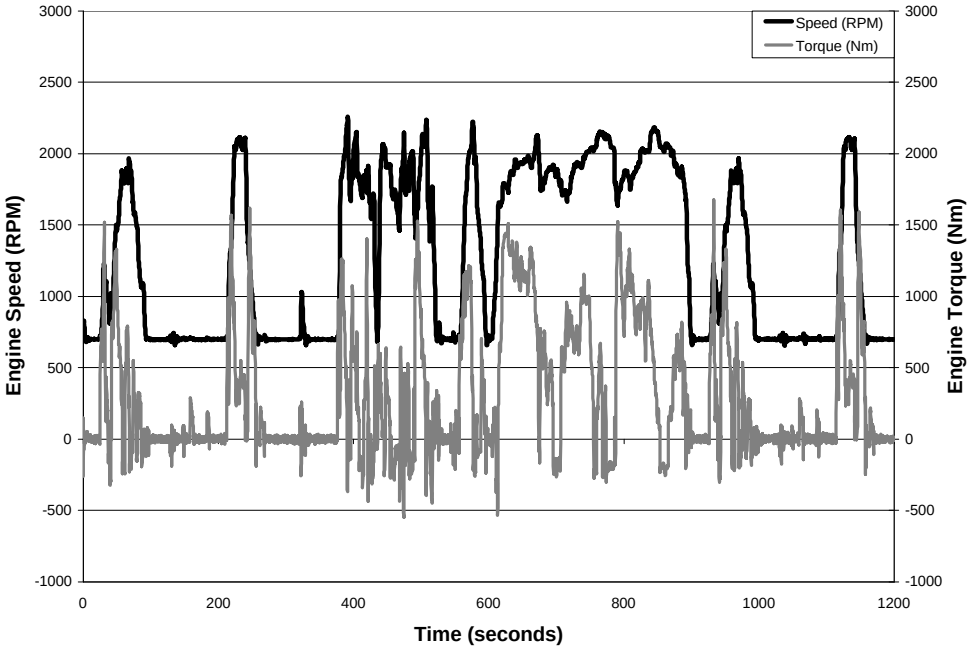

Figure 2: Engine speed and load for a 10.8 liter Cummins during a FTP test cycle.

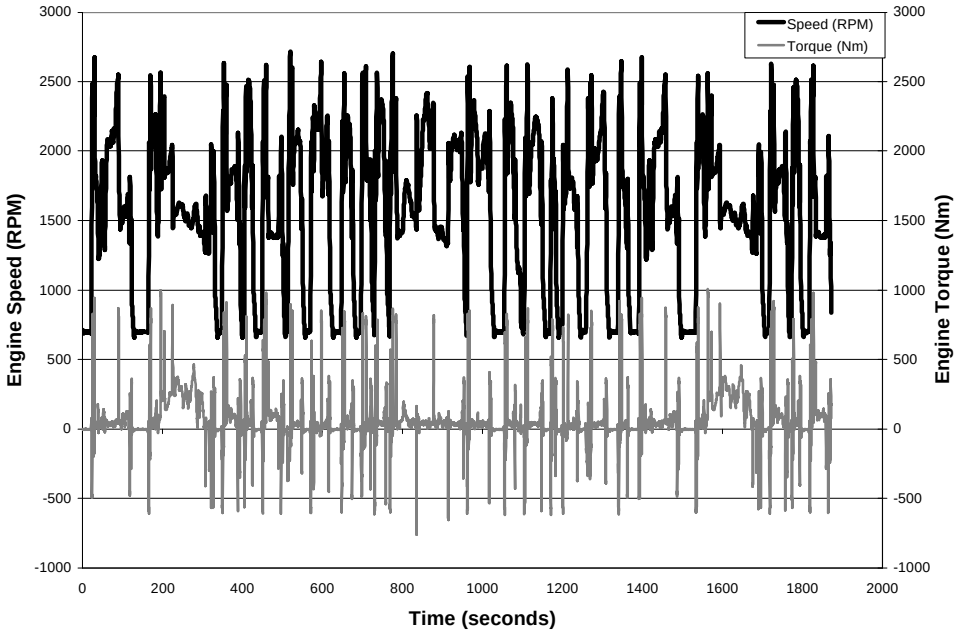

Figure 3: Engine speed and load for a 7.3 liter Navistar for a WVU FTP 75 test cycle.

3.1.1.2 Exhaust Dilution and Instrumentation

Exhaust gases were ducted from the engine to the primary dilution tunnel through a five inch (12.7 cm) diameter insulated carbon steel pipe approximately 26 feet (7.9m) long. The primary dilution tunnel was 18 inches (45.7 cm) in diameter, incorporating a mixing orifice to promote mixing of the engine emissions with the temperature conditioned test cell air. Sampling probes were placed radially from the longitudinal centerline to form a sampling plane that was perpendicular to the flow 180 inches (457 cm) down stream of the tunnel opening. Analyzers sampling from this location measured HC, oxides of nitrogen (NO_x), carbon monoxide (CO), carbon dioxide (CO_2), and TEOM PM. The volume of mixed air and exhaust was controlled by a critical flow venturi operating in a choked flow condition.

The venturi was set at 1000 cfm and 2400 cfm for the Navistar and Cummins, respectively. The diluted exhaust was pulled through the venturi by a blower and then vented to the atmosphere. By injecting a known amount of propane into the tunnel and measuring the amount recovered by the HC analyzer, the tunnel integrity and accuracy was tested. Sampling probes and sample lines were heated to prevent condensation of moisture and hydrocarbons while transferring diluted exhaust gases to the analyzers.

The HC analyzer was a model 402 flame ionization detector made by Rosemount Analytical, Inc. The NO_x analyzer used was a Rosemount Analytical, Inc chemiluminescent model 955. The CO analyzer used was a Rosemount Analytical, Inc model 880A non-dispersive infrared unit. The CO_2 analyzer used was also a non-dispersive infrared instrument, however, some tests used a Beckman Industrial model 868, and other tests used a Rosemount Analytical, Inc model 880A. All gas instruments were calibrated and set to zero air and spanned with calibration gases before testing.

To collect PM in spirit of the EPA regulations, as specified in Title 40 of the Code of Federal Regulations [2], a sample of diluted exhaust gas was pulled from the sampling plane in the primary dilution tunnel into a secondary dilution tunnel. The sample was passed across a pair of 70 mm diameter microfiber filters in series at a set volumetric flow rate via a mass flow controller and vacuum pump. The filters used were Pall-Gelman Science “Pallflex Fiberfilm” T60A20 heat resistant borosilicate glass fiber coated with TFE, as seen in figure 6. Figures 4 and 5 illustrate the cartridge that contained the filters during the test cycle.

Figure 4: The 70 mm diameter PM filter cartridge disassembled. This filter module was used for the conventional, EPA-style, PM collection.

Figure 5: The PM filter cartridge assembled.

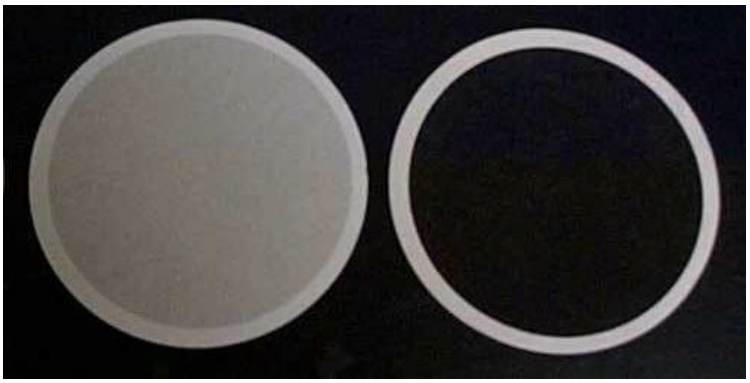

Figure 6: Typical used secondary (left) and primary (right) PM filters.
This photo shows the inefficiency of the T60A20 filter by the
amount of PM collected on the secondary filter.

No secondary dilution was necessary, as the sample filter face temperature remained below 125°F (52°C). The set volumetric sample rate was five scfm (141 lpm). The filters were conditioned in an environmentally controlled chamber where the temperature remained at 70°F +/- 10°F and the relative humidity was constrained to 50% +/- 10%. The filters were conditioned and weighed before and after each test with a Cahn C-32 microbalance to calculate the collected PM mass. The PM concentration was calculated by dividing the collected PM mass by the total volume passed through the filter set during the test cycle.

Figure 7: The microbalance used weigh conventional PM filters
before and after each test.

The TEOM model 1105 was used to sample in two locations. The first location was at the sampling plane in the primary dilution tunnel, see figures 8 and 9 for illustration. The second location was at the bottom of the secondary dilution tunnel, above the PM filters. The sample location from the

secondary tunnel is illustrated in figures 10 and 11. This second location was to investigate the possible effect of concentration or pressure variations on TEOM data.

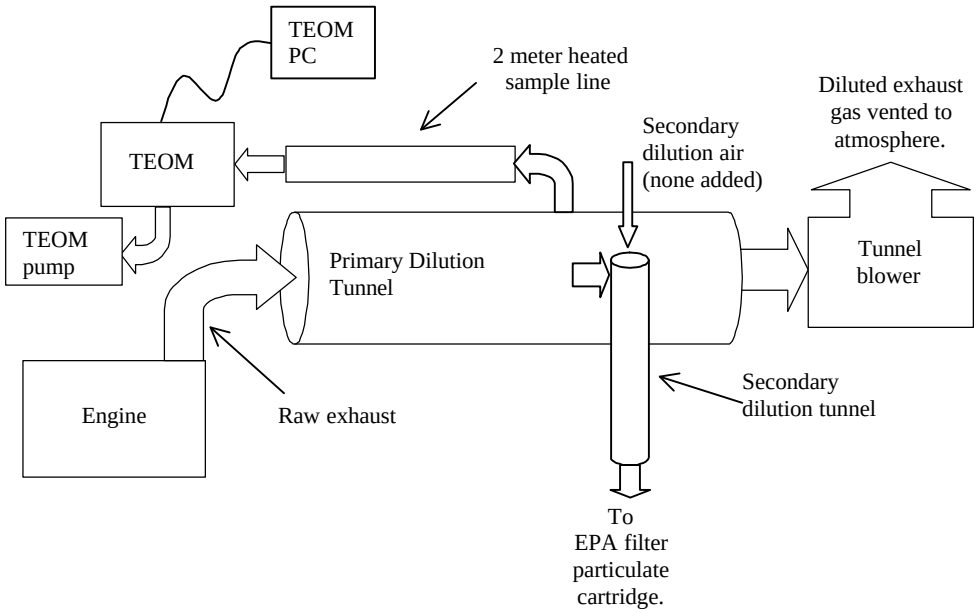

Figure 8: The particulate sampling system with the TEOM sampling from the primary dilution tunnel.

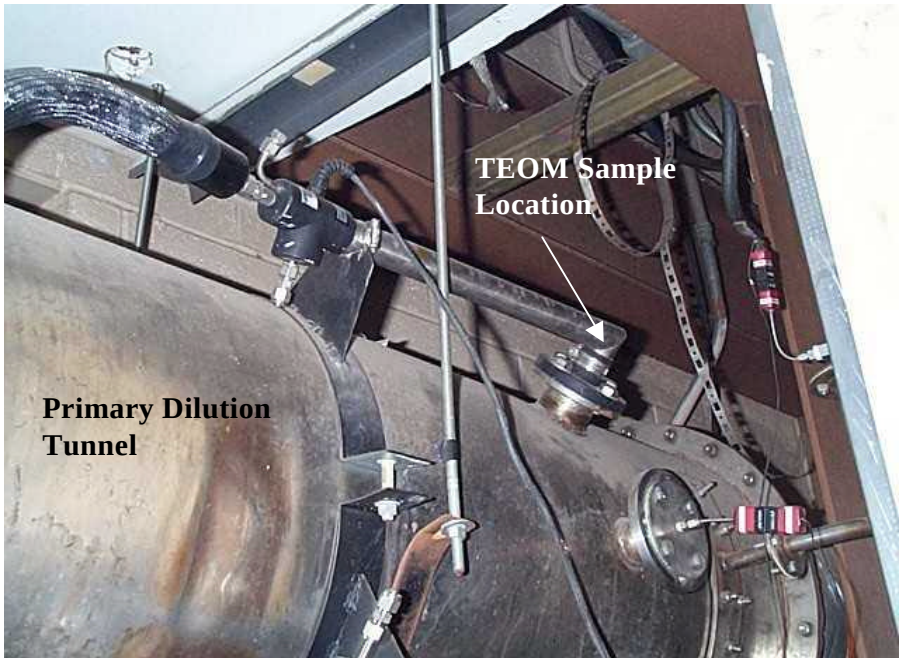

Figure 9: The TEOM sampling location on the primary dilution tunnel.

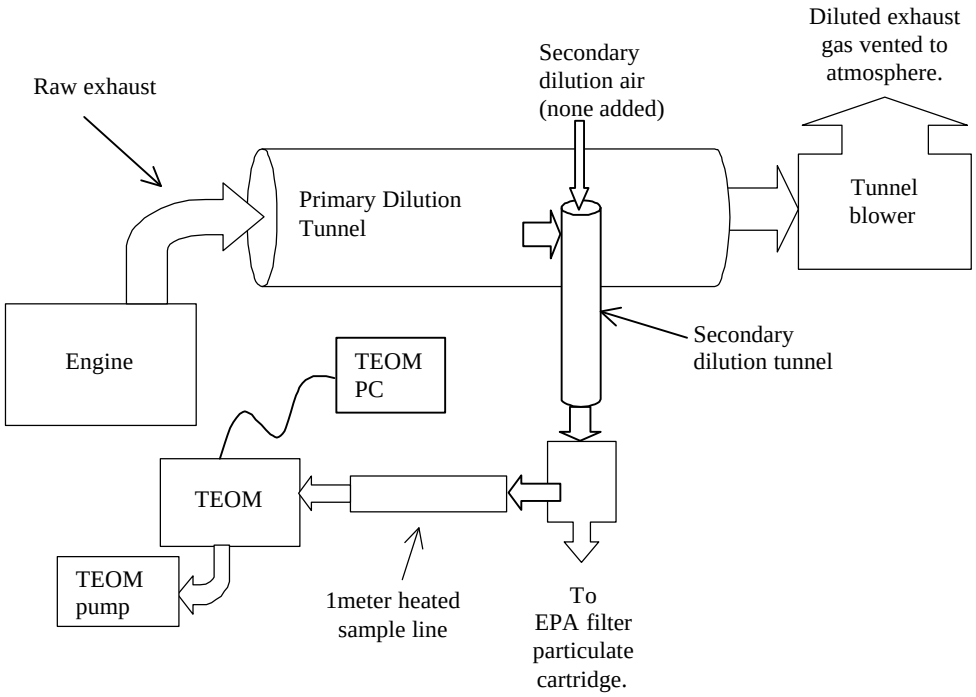

Figure 10: The particulate sampling system with the TEOM sampling from the secondary dilution tunnel.

Figure 11: The TEOM sampling location on the secondary dilution tunnel

3.1.2 Transportable Heavy Duty Vehicle and Emissions Laboratory

3.1.2.1 Vehicle and Chassis Dynamometer

The chassis dynamometer was designed to test medium to heavy-duty highway vehicles [14]. The chassis dynamometer utilized rollers to support the drive axle of a vehicle as with a conventional chassis dynamometer. However, power was taken from the vehicle through hub adapters bolted to each side of the driven axle on the wheel flanges. The rollers were coupled to ensure even torque distribution between left and right wheels. Road loads were simulated through a combination of flywheels and eddy current absorbers. The flywheels were used to simulate the inertia of the vehicle, while the eddy current absorbers simulated additional forces due to acceleration. The vehicle speed points came from the Central Business District (CBD) test cycle, as depicted in figure 12. The vehicle used for the test sequence was a transit bus manufactured by Collins. Specific information on the test vehicle can be found in table 2. Although illustrations 13 and 14 do not show the transit bus used, illustrated is a typical vehicle operation on the portable heavy-duty chassis dynamometer

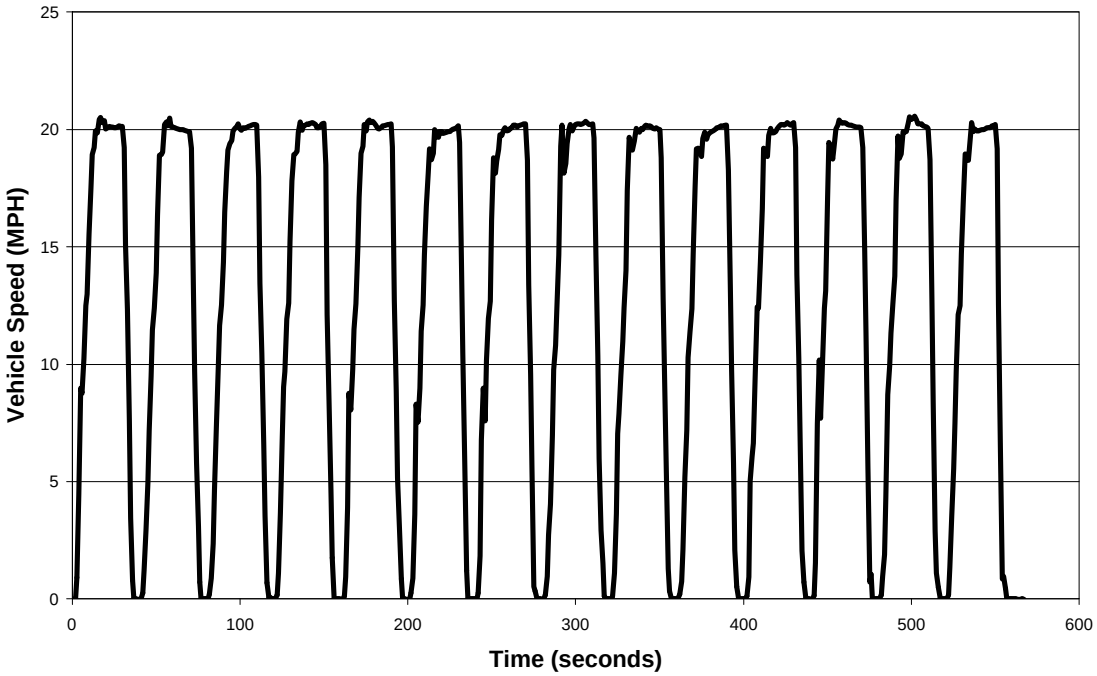

Figure 12: Measured vehicle speed for a Collins transit bus driving the CBD cycle on the transportable laboratory.

Table 2: Transit bus tested on the mobile emission laboratory.

Fleet Owner	Denver Regional Transit District
Vehicle Type	Transit Bus
Vehicle Manufacturer	COLLINS
Vehicle Model Year	1997
Gross Vehicle Weight	18780 lb.
Vehicle Total Curb Weight	14525 lb.
Vehicle Tested Weight	17914 lb.
Odometer Reading	18700 miles
Transmission Type	4-speed Automatic
Number of Axles	2
Engine Type	Cummins B5.9 - 175
Engine Displacement	5.9 Liter
Number of Cylinders	6
Engine Rated Power	175 hp
Fuel	D2

Figure 13: Although this illustration does not show the transit busses used, illustrated here is a typical vehicle operation on the portable heavy-duty chassis dynamometer.

Figure 14: Typical routing of vehicle exhaust into the emissions trailer of the mobile laboratory.

3.1.2.2 Emission Dilution and Instrumentation

The dilution system in the THDVETL parallels the design in the EERL and its description can be found in section 3.1.1.2. However, the transportable laboratory does not have the capability of conditioning the air used for combustion and dilution. The HC, NO_x, and CO analyzers were the same models as used in the Engine and Emission Research Center and their descriptions can be found in section 3.1.1.2. The CO_2 analyzer used was a Rosemount Analytical, Inc model 880A non-dispersive infrared unit. Particulate sampling was also parallel in design and operation as the system used at the EERL. However, the TEOM was only setup to sample at the bottom of the secondary dilution tunnel as illustrated in Figure 10.

3.2 Description and Setup of the TEOM

3.2.1 Description

The essential component to the TEOM is a hollow, tapered, cantilever element, which is forced to oscillate at its natural frequency via magnetic field plates and a feedback system. The filter is mounted onto the free end of the cantilevered, tapered element. An internal volumetric flow controller regulates a constant sample of diluted exhaust gas pulled across the filter. Simplistically, the element and filter system can be represented by a spring-mass system, where a change in mass correlates to a change in frequency. As the filter weight changes due to PM accumulation, the frequency of the element's oscillation changes. The TEOM measured the frequency of the tapered element oscillation

and calculated a new filter weight. A new weight was calculated approximately every one fifth of a second.

The TEOM was controlled by a PC via counter timer and analog/digital input output boards. These boards are managed through TEOMPLUS® software supplied by Rupprecht & Patashnick. This software provides an easy interface for instrument set up and data acquisition. Critical instrument set up parameters include sample volumetric flow rate and internal and external sample line temperatures. User defined data acquisition variables include sampling rate and time window averaging.

3.2.2 TEOM Setup

The instrument was placed on a stable shelf in a position as close as possible to the sampling location. A Pentium-class IBM compatible PC was used to control the sampling unit. Two printed circuit boards were installed into the PC to interface with the TEOM. The Robotrol data acquisition board was used for data and communication while the R&P counter timer board controls frequency of data acquisition. The jumper on the counter timer board was set to position E which corresponds to a data cycle time of 0.1048576 seconds. This jumper setting was chosen because the PC could not update the time axis on the display screen without affecting TEOM acquisition sampling at a faster data cycle time. TEOM setup parameters were established in the instrument configuration file and the user configuration file. The instrument configuration file, "1105.INS", configuration file, "1105P.CON", and TEOM channel assignments are described in Appendix A. At the EERL, the TEOM total mass and TEOM mass concentration data were acquired in parallel with other real time analyzers and engine parameters through the existing data acquisition system. Also, for use at the EERL, the TEOM acquisition was started, stopped, and reinitialized by sending TTL level signals to user digital input channels of the user I/O port. The pin designations for the user I/O port and logic for remote collection can be found in Appendix A. Collecting data at the portable emission laboratory was done manually and data were acquired with the TEOM PC. For all testing in this study, a 3 second moving window average was applied to the data. This averaging was applied by the TEOM and the duration can be user defined in the configuration files. The significance of data averaging was not investigated because of the direct influence on system response. Figure 15 reveals the internals of the TEOM unit.

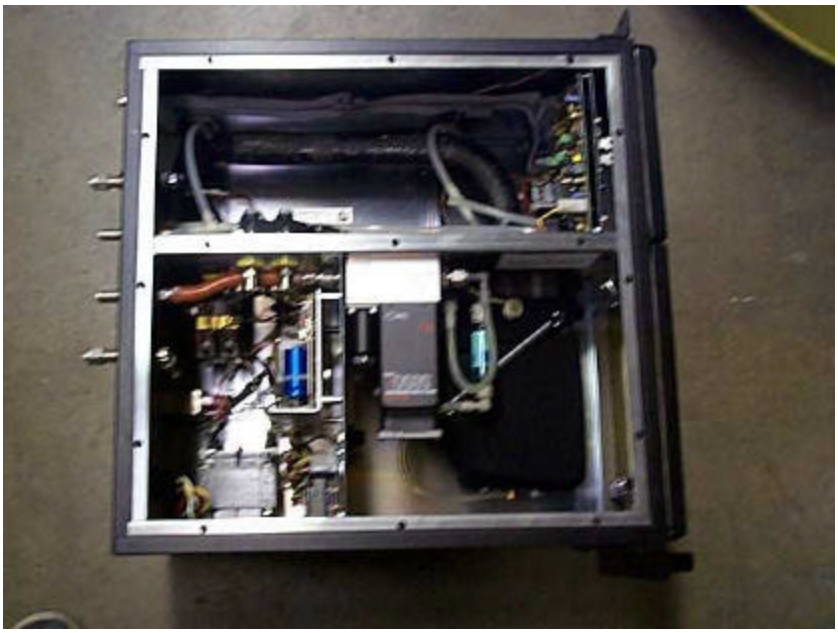

Figure 15: Internal view of the TEOM showing the mass flow controller, amplification boards, TE housing, and the internal sample line.

Figure 16: The front panel of the TEOM. Although the results were not verified, the foam that the TEOM was resting upon was to help eliminate external vibration.

4 Experimental Approach

4.1 Temperature Effects

To investigate and validate further the effect of sample tube temperature on TEOM data, the TEOM end-of-test mass was compared to the conventional PM collection and real-time TEOM data were scrutinized. The first phase of tests involved exploring four temperature set points while the flow rate was held constant. Results were compared by using flow normalized end-of-test particulate mass, referred to as mass concentration (mc), reported in milligrams of PM per cubic meter of sample. The end-of-test particulate mass used for calculation were the reported value from the TEOM and the conventional PM gravimetrically measured mass. The end-of-test particulate mass was then divided by the total volume of sample that was passed across the filter. The sample volume was measured and controlled by separate electronic volumetric flow controllers for each collection method. No corrections for background PM were applied to the data. It was assumed that an equivalent amount of background PM was collected by each method. Further more, the error stacking would add randomness to the study. Equations 1 and 2 represent the formulas used to calculate mass concentration for the conventional and TEOM measurement methods respectively.

$$Conventional_{mc} = \frac{Mass_{filter\_post-test} - Mass_{filter\_pre-test}}{Volume_{conventional}} \quad (1)$$

$$TEOM_{mc} = \frac{End\_of\_Test\_Mass_{TEOM}}{Volume_{TEOM}} \quad (2)$$

The comparisons of TEOM-to-conventional PM values were made by using percent difference from conventional PM, equation 3.

$$PercentDifference = \frac{(Conventional_{mc} - TEOM_{mc})}{Conventional_{mc}} \times 100\% \quad (3)$$

For these evaluations, a percent difference from conventional PM value of one hundred percent was desirable. To quantify the overall variability in TEOM results, a t-distribution [17] was compiled to calculate the 99% confidence level for the temperature data taken with the Navistar engine. This method assumes that the distribution of end-of-test TEOM mass data distribution is Guassian. Furthermore, to increase the sample size, the 99% confidence level was calculated by treating the data as a single set, or videlicet, assuming the effect of TEOM sample temperature has a negligible effect on the statistical confidence value. This method served as a conservative representation of uncertainty due to the true effect of TEOM sample temperatures on PM collection. Conventional PM concentration

values provided a baseline for the validation of the TEOM instrument. However, the primary purpose of the instrument is to measure real-time PM, so a criterion was needed to evaluate this feature.

Two mass vectors describe the filter loading. One positive vector represents VOC, moisture, and particulate collecting on the filter. One negative vector represents VOC and moisture coming off the filter. During light loading conditions, such as idle or no-load conditions, the VOC and moisture that had built up during heavy loading continued to evaporate from the filter. This exodus of mass from the filter surfaced in the data as a negative mass change. Although previous work [7-11] suggests that the negative mass rate data trends are real phenomena, it is generally thought that the ideal real-time PM results should only be positive. This is a semantic debate, which rests in the definition of PM and its creation. To judge the overall negative mass rate occurrence of the data, the real-time results were separated into positive values and negative values. These two fractions were numerically integrated to provide values for the total amount of positive and "negative" mass collected. The summation of these two integrated values would be the total mass collected on the filter during the test. The ratio of the positive mass over the negative mass yielded one effective criterion for the evaluation of real-time results. A high positive-to-negative mass ratio was desirable. For these temperature sweeps, a flow rate of 3 lpm was chosen as per the previous work performed by Okrent [8] and Shore [7].

4.2 Flow Effects

Using the temperature set point that gave the best compromise of conventional PM agreement and real-time results from the section above, a sweep of four TEOM sample flow set points was taken holding the temperature set point constant. The end-of-test TEOM results were compared with conventional PM filter collection results. A t-distribution was calculated, using the entire Cummins engine set. The temperature and flow studies were regarded as one set of consistent data to calculate the 99% confidence level. By grouping all Cummins engine tests together in the 99% confidence calculation, it is assumed that the effects of temperature and flow variations are negligible in the statistical confidence value. In addition, the real-time data were evaluated in the same manor as the temperature effect tests outlined above.

4.3 Sampling Location Effects

The sampling location was changed from the primary dilution tunnel to the secondary dilution tunnel, again comparing TEOM results with conventional PM filter collection results and real-time data evaluation was conducted in the same manor as the temperature effect tests outlined above. The TEOM temperature and flow set points that yielded the best results were used to compare the two sampling locations.

4.4 Filter Conditioning

Five types of tests were performed to investigate the effect of filter pre-conditioning on start up delay after filter replacement. Each test consisted of a different type of filter storage, or conditioning. For bag, chamber, room, and 100% relative humidity (RH) conditioning, a new filter was placed in the TEOM and sampling was started immediately. For each of these conditioning criteria, filters were allowed to condition for at least 24 hours. Bag conditioned filters were stored in the R&P Company supplied resealable bag containing a silica gel package. Chamber conditioned filters were stored in the same environmental chamber where conventional PM filters were stored. Temperature and humidity readings were 22°C and 45% RH respectively. Room conditioned filters were allowed to condition in a petri dish in the ambient temperature and humidity conditions at 21°C and 30% RH. Filters conditioned at 100% RH were stored at room temperature in a petri dish containing a damp wick. The saturated tests were conducted by placing a drop of water on the filter while installed in the TEOM unit, then immediately starting sampling. The TEOM was set to sample at 50°C and 2 lpm during all tests except the 100% RH tests. In the 100% RH tests, results from 50°C, 2 lpm settings were compared to 40°C, 3 lpm settings.

4.5 Effect of Filter Type

There are two types of filter media popularly used in particulate collection, the Pall-Gelman Science "Pallflex Fiberfilm" T60A20 and TX40. The only filter medium used in this research was a conventional PM filter was the T60A20. The efficiency of the conventional PM filter method was not questioned due to its two stage series filter design. The TX40 is the most common filter to use in the TEOM due to its higher initial filtration efficiency. Both filters are very similar in material and construction; their properties are outlined in tables 3 and 4. The application of T60A20 filter use in the TEOM was tested against the more commonly used TX40. The TEOM temperature and flow set points that yielded the best results in the previous experiments were used to compare the two filter types.

Table 3: T60A20 filter properties [15].

Filter Media	Heat resistant borosilicate glass fiber coated with fluorocarbon (TFE).
Typical Thickness	8 mils (0.20 mm)
Typical Weight	3.4 mg/cm^2
Typical Air Flow Rate	180 l/min/cm^2 at 10 psi
Maximum Operating Temperature - Air	315.5° Celsius (600 F)

Table 4: TX40 filter properties [15].

Filter Media	Borosilicate microfibers reinforced with woven glass cloth and bonded with PTFE.
Typical Thickness	7 mils (0.17 mm)
Typical Weight	5.0 mg/cm^2
Typical Air Flow Rate	68 l/min/cm^2 at 10 psi
Maximum Operating Temperature - Air	260° Celsius (500 F)

4.6 Real Time Observations

The use of the TEOM as a real-time tool was investigated through graphical analyses by comparison of other real-time analyzers and engine parameters such as HC, CO, NO_X, and torque. Due to the unique response time of each instrument, it was necessary to time shift each emission individually. A Microsoft Visual Basic program was written to find an optimal time shift. The code for the program can be seen in Appendix B. The programs' design was inspired by Messer's [18] work at WVU. Messer proposed that emissions increase with power and that the correlation between the two will be at a maximum when emissions are shifted correctly. Correlating the entire length of the test compensates for exhaust flow rate variations and thus inconsistency in time shift. The correlation equation is as follows:

$$Correlation_{x,y} = \frac{\frac{1}{n}\sum_{j=1}^{n}(x_j - \bar{x}_j)(y_j - \bar{y})}{s_x s_y} \quad (4)$$

Where, in equation 1, *x* and *y* are vectors of data. The numerator of equation 4 is the covariance, and the denominator is the product of the standard deviations. The *y* vector was moved in relation to *x* for every time shift and correlation values, the result from equation 4, were recorded. In an effort to account for engine and fuel variations, it was deemed necessary to simplify these data by normalizing each emission and engine parameter by dividing each real-time point by the respective test average value.

5 Data, Results, and Discussion

5.1 Temperature Effects

5.1.1 Navistar

The general scope of this testing was to vary the temperature settings of the TEOM while keeping flow constant. There was no attempt to match the sample temperatures of the TEOM directly to the sample temperatures of the conventional PM filters. Two engines were used to evaluate the effect of temperature settings on the TEOM particulate sampler. The first tests were conducted on the Navistar engine. The engine was run through an FTP speed-load cycle to bring the engine and tunnel to operating temperature before data were taken. Twelve FTP speed-load cycles were run back to back with a nominal engine off time of 10 minutes between tests. Three FTP speed-load cycles were used for each TEOM sample tube temperature set point. The TEOM TE housing, external and internal sample tube temperature set points were 35°C, 40°C, 50°C, and 60°C. To remain consistent and identify new filter collection efficiency, a new TEOM filter was used at the start of every test set. It is conceded that new filters may pass some PM species before deposition increased capture efficiency. Only on this set of experiments was the initial test reported and included in calculations. The coefficient of variance (COV) of the conventional PM flow normalized data were 2.6%, proving data viability. The COV for the average air temperature for the conventional PM sampling system was 3.3%, proving the consistency of the sample temperatures.

For the first set of three tests, the TE housing, external and internal sample tube temperatures were set to 35°C, resulting in a sample air temperature of 34°C. A new TX40 filter was installed in the TEOM before the test series began. The percent difference calculated in Table 5 was based on the deviation of the TEOM value from the conventional PM value. Figure 17 displays the TEOM to Conventional PM collection ratio.

Table 5: Results from the 35°C TEOM set point on the Navistar.

Test Number	Conventional PM Average Air Temperature (°C)	TEOM Average Air Temperature (°C)	Conventional PM Concentration (mg/m^3)	TEOM Concentration (mg/m^3)	Percent Difference from Conventional
1	36	34	1.16	0.90	22.41%
2	38	34	1.16	1.06	9.06%
3	39	34	1.19	1.16	2.89%

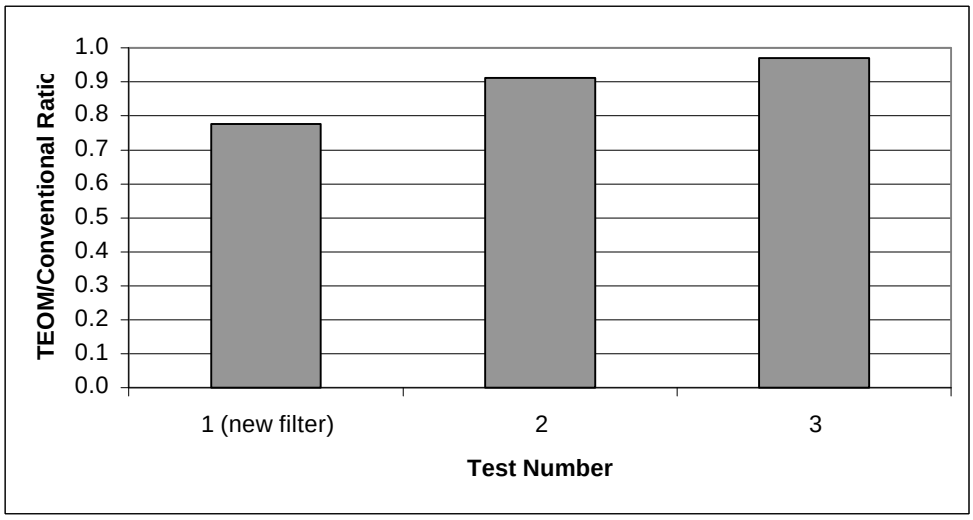

Figure 17: TEOM/conventional PM ratio for the 35°C TEOM set point on a Navistar 7.3 liter diesel. The improvement in filter efficiency was evident as the test sequence proceeds due to PM loading.

The first test in this set displays the poor collection efficiency relative to the conventional PM filters. The conventional PM filter system utilizes a two stage filter system, where as the TEOM only uses a single stage. For the second set of FTP tests, the TEOM temperatures were set to 40°C, resulting in a sample air temperature of 38°C. A new TX40 filter was installed in the TEOM before the test series began. Results from this test set are shown in table 6. Figure 18 shows a bar graph of the TEOM to Conventional PN collection ratio.

Table 6: Results from the 40°C TEOM set point on a Navistar 7.3 liter diesel engine.

Test Number	Conventional PM Average Air Temperature (°C)	TEOM Average Air Temperature (°C)	Conventional PM Concentration (mg/m^3)	TEOM Concentration (mg/m^3)	Percent Difference from Conventional
4	38	39	1.21	0.83	32.0%
5	39	39	1.20	0.95	20.8%
6	40	39	1.21	1.03	14.4%

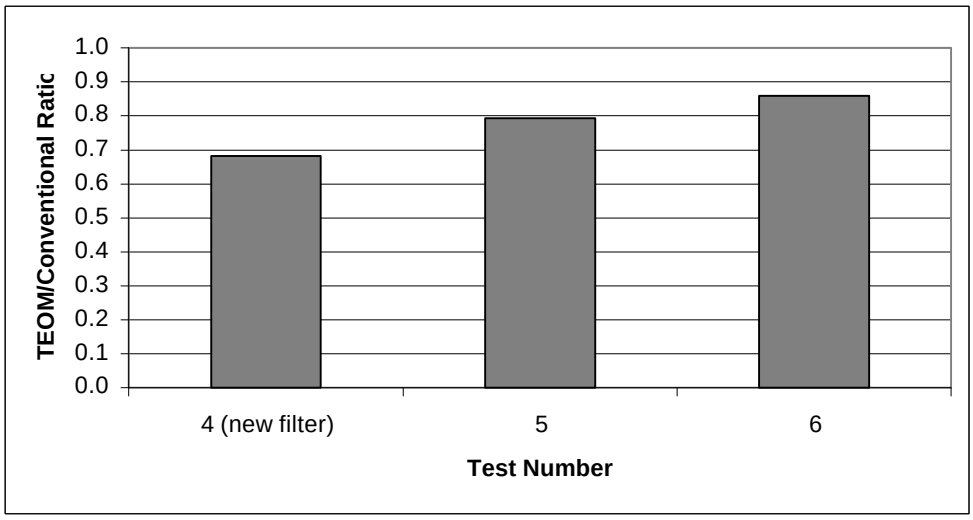

Figure 18: TEOM/conventional PM ratio for the 40°C TEOM set point on a Navistar 7.3 liter diesel. The improvement in filter efficiency was repeats as the test sequence proceeded due to PM loading.

Again, the relative initial inefficiency of the TEOM filter was apparent in the first test of this set. The rise in TEOM sampling temperature caused an increase in the average error from 11.45% to 22.40%. The error increase could possibly be due to the lack of moisture and VOC collecting on the TEOM filter due to the increase in temperature. For the third set of FTP tests, the TEOM temperatures were set to 50°C, resulting in a sample air temperature of 48°C. A new TX40 filter was installed in the TEOM before the test series began. Results for the third set are catalogued in table 7. TEOM to Conventional PM collection ratios are shown in figure 19.

Table 7: Results from the 50°C TEOM set point on a Navistar 7.3 liter diesel engine.

Test Number	Conventional PM Average Air Temperature (°C)	TEOM Average Air Temperature (°C)	Conventional PM Concentration (mg/m^3)	TEOM Concentration (mg/m^3)	Percent Difference from Conventional
7	37	47	1.27	0.69	46.0%
8	39	48	1.20	0.98	18.0%
9	38	48	1.21	0.98	19.1%

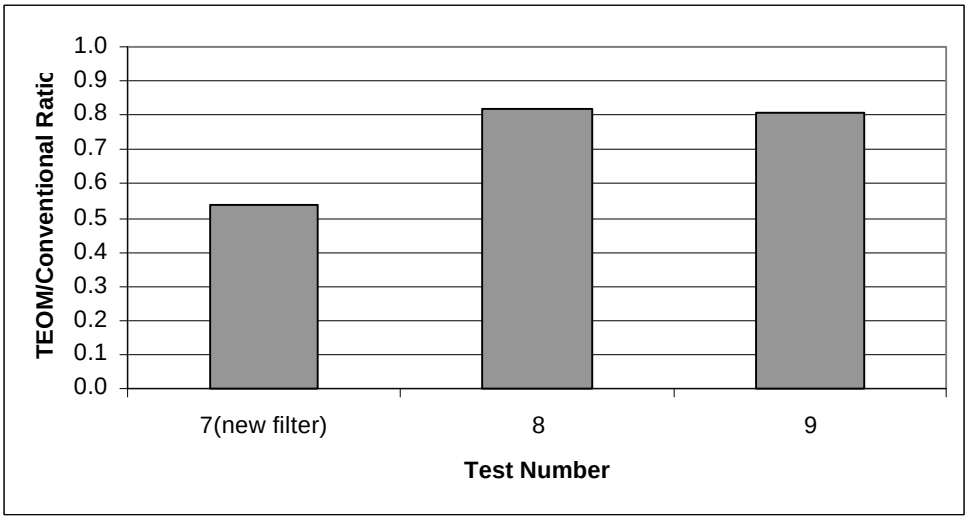

Figure 19: TEOM/conventional PM ratio for the 50°C TEOM set point on a Navistar 7.3 liter diesel. The TEOM continues to deviate from conventional PM filters as temperature increased.

As expected, the first test in the series had a significantly higher error than the other two tests. The rise in TEOM sampling temperature caused an increase in the average error from 22.40% to 27.70%. The forth and final set of three tests, the TEOM temperatures were set to 60°C, resulting in a sample air temperature of 56°C. A new TX40 filter was installed in the TEOM before the test series began. Table 8 displays data captured from this set, while the TEOM to Conventional PM collection ratio is displayed in figure 20.

Table 8: Results from the 60°C TEOM set point on a Navistar 7.3 liter diesel engine.

Test Number	Conventional PM Average Air Temperature (°C)	TEOM Average Air Temperature (°C)	Conventional PM Concentration (mg/m^3)	TEOM Concentration (mg/m^3)	Percent Difference from Conventional
10	36	56	1.24	0.11	91.3%
11	38	56	1.23	0.77	37.3%
12	39	56	1.22	0.96	21.4%

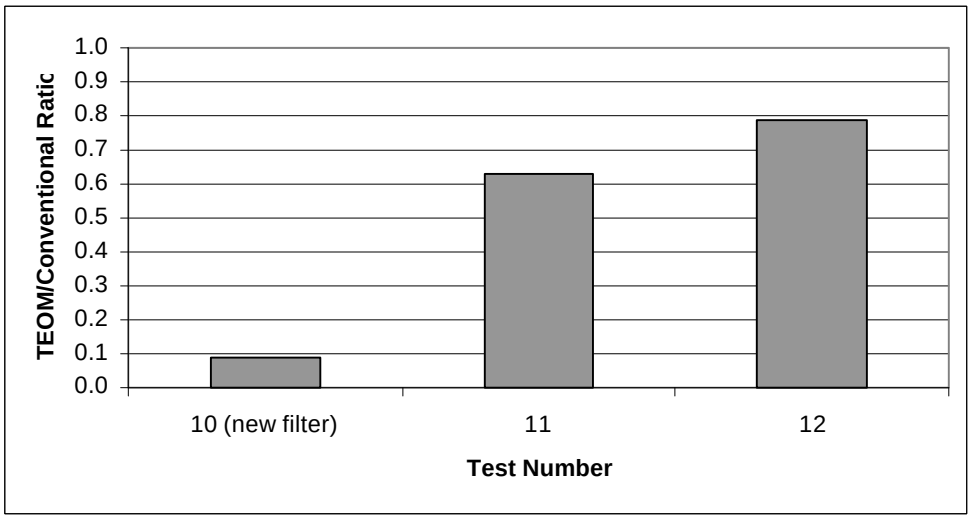

Figure 20: TEOM/conventional PM ratio for the 60°C TEOM set point on a Navistar 7.3 liter diesel.

The average error continued to increase with temperature, from the previous test sequence average value of 27.70% to 49.97%. A trend in initial collection efficiency becomes apparent. As the temperature increased, the error, or percent difference from conventional, associated with the initial collection increased rapidly, looking as if it were following an exponential trend as shown in figure 21.

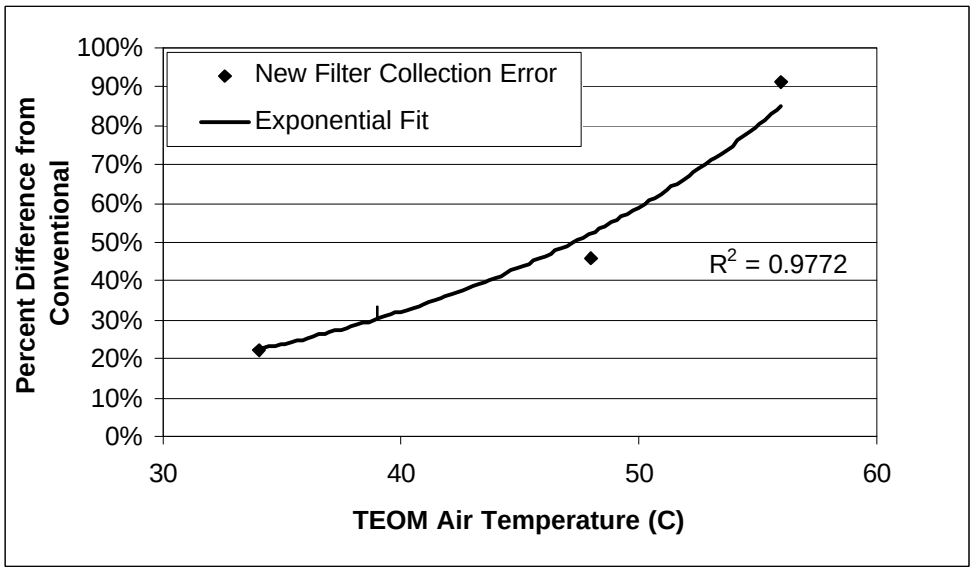

Figure 21: New filter collection error increased as TEOM air temperature increased with an apparent expontial relationship.

This exponential trend shows the true collection characteristics of the filter. The second and third tests in each series may not show this trend due to the ability of the moisture and VOC being absorbed readily into the PM present on a soiled filter. On average, the first filter captured 40% less

than the third filter. A filter cartridge that housed two filters would improve the initial collection efficiency. The 99% confidence of the conventional PM concentration over the 12 sample set was ± 2.3 %, or 1.21±0.028 mg/m^3. Assuming that the variation in TEOM sampling temperature was negligible in the confidence value, the 99% confidence of the TEOM concentration over the 12 sample set was ±28.0%, or 0.868±0.243 mg/m^3.

5.1.2 Cummins

The second set of tests was conducted on the Cummins 10.8 liter DI diesel engine. The engine was run through an FTP cycle to bring the engine and tunnel to operating temperature before data were taken. Nine FTP speed-load cycles were run back to back with a nominal heat soak time of 10 minutes between tests. When the TEOM filter was changed, an FTP was run to condition the filter in an attempt to minimize the filter capture efficiency variability. These conditioning FTPs were not included in the analysis of the data. However, even the second test on a new TEOM filter will show effects of efficiency changes. Three FTP speed load cycles were run for each TEOM temperature. These set points were 30°C, 40°C, and 50°C. The COV% of the conventional PM flow normalized data was 1.3%, proving data viability. The COV% for the average air temperature for the conventional PM sampling system was 4.1%, proving the consistency of the sample temperatures. The average relative humidity of the ambient air for the duration of the test series was 25%.

For the first set of FTP tests, the TEOM temperatures were set to 30°C, resulting in a sample air temperature of 30°C. Data is tabulated in table 9. Figure 22 is a bar chart showing the TEOM to Conventional PM collection ratio for each run.

Table 9: Results from the 30°C TEOM set point on a Cummins 10.8 liter diesel engine.

Test Number	Conventional PM Average Air Temperature (°C)	TEOM Average Air Temperature (°C)	Conventional PM Concentration (mg/m^3)	TEOM Concentration (mg/m^3)	Percent Difference From Conventional
1	38	30	1.24	1.11	10.6%
2	39	30	1.24	1.14	8.3%
3	39	30	1.26	1.14	9.2%

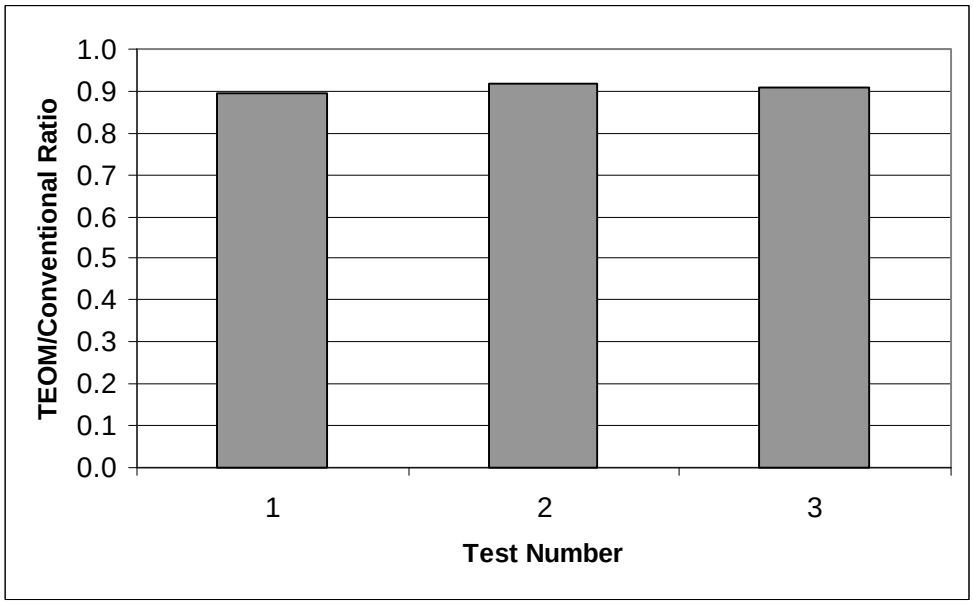

Figure 22: TEOM/conventional PM ratio for the 30°C TEOM set point on a Cummins 10.8 liter diesel engine. A test cycle was performed prior to test 1 shown above. This provided and increased consistency (COV% of 1.28%) during this test series.

The TEOM gives repeatable results with a preconditioned filter. The Cummins 30°C results were not as close as the Navistar 35°C results. However, for the Cummins tests, there was almost a 10°C difference between TEOM and conventional PM temperatures. For the Navistar tests, the difference between TEOM and conventional PM temperatures was only 4°C. It was the experience of the author as the TEOM sample temperature reached the temperatures of the conventional sample, the difference between TEOM and conventional PM decreased. For the second set of FTP tests, the TEOM temperatures were set to 40°C, resulting in a sample air temperature of 39°C. The following table (10) and chart (figure 23) display data from these tests.

Table 10: Results from the 40°C TEOM set point on a Cummins 10.8 liter diesel.

Test Number	Conventional PM Average Air Temperature (°C)	TEOM Average Air Temperature (°C)	Conventional PM Concentration (mg/m^3)	TEOM Concentration (mg/m^3)	Percent Difference From Conventional
4	39	39	1.22	1.11	8.4%
5	35	39	1.20	1.10	8.6%
6	36	40	1.24	1.13	8.3%

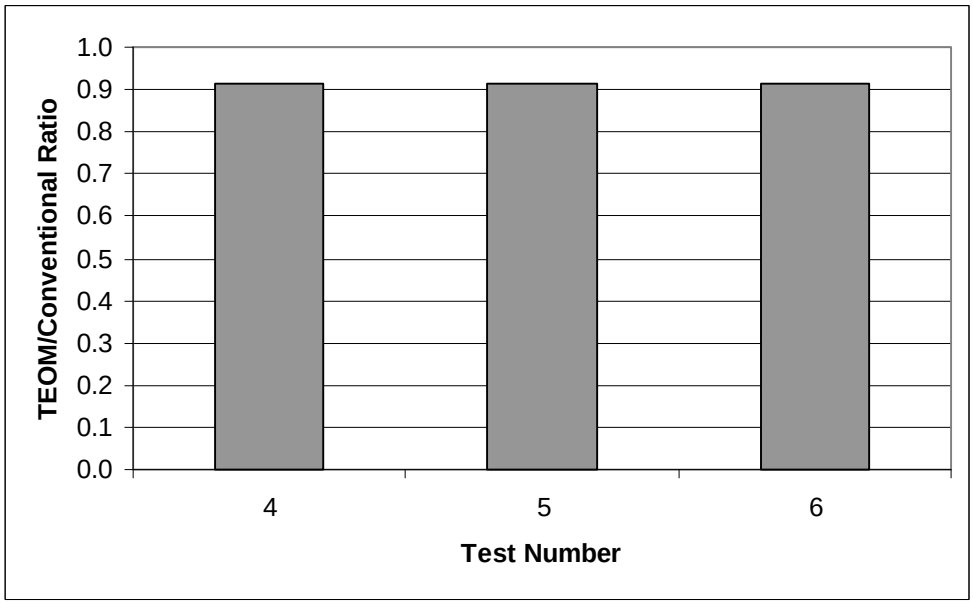

Figure 23: TEOM/conventional PM ratio for the 40°C TEOM set point on a Cummins 10.8 liter diesel engine. This series proved to be a very consistent set of tests, COV% of the ratio was 0.15%.

The final set of tests was taken at a sample path temperature of 50°C, resulting in a PM sample temperature of 48°C. A test was run on a new filter for conditioning purposes. The difference between convention and TEOM measurement increased from an average percent difference of 8.43% to an average percent difference of 20.53% respectively. In addition, test variability increased. The TEOM COV at 40°C was 0.2% while TEOM COV at 50°C was 5.2%. Conventional PM measurement COV remained stable between the two test batteries, ruling out engine variability. Table 11 and figure 24 reflect the results for these 50°C tests. Figure 25 shows all the percent difference values for the Cummins temperature testing to reflect the increase at 50°C.

Table 11: Results from the 50°C TEOM set point on a Cummins 10.8 liter diesel engine.

Test Number	Conventional PM Average Air Temperature (°C)	TEOM Average Air Temperature (°C)	Conventional PM Concentration (mg/m^3)	TEOM Concentration (mg/m^3)	Percent Difference From Conventional
7	36	48	1.25	0.94	25.3%
8	39	48	1.24	1.01	18.3%
9	39	48	1.24	1.02	18.1%

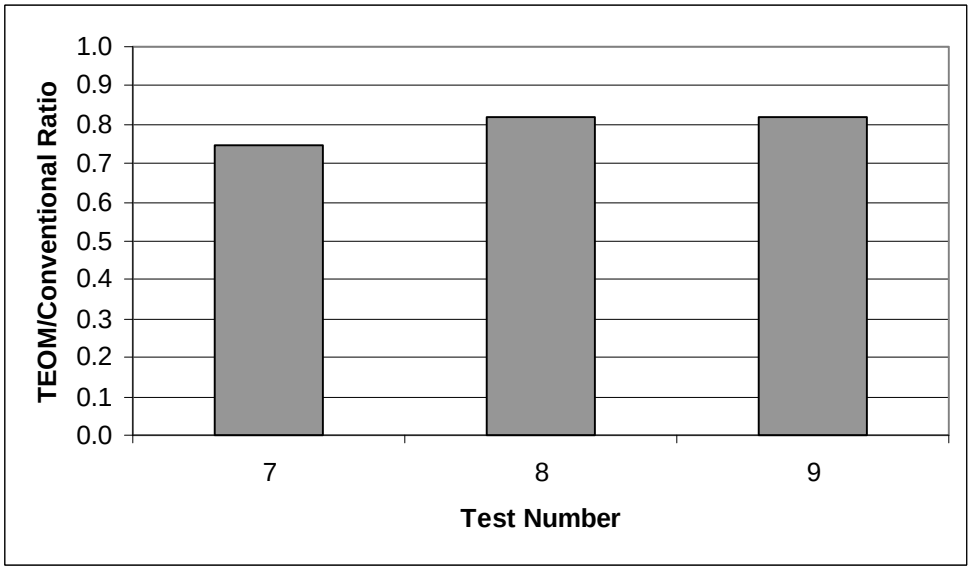

Figure 24: TEOM/conventional PM ratio for the 50°C TEOM set point on a Cummins 10.8 liter diesel engine. As with the temperature test on the Navistar engine, a 50°C sampling temperature yielded a decrease in the TEOM/conventional PM ratio.

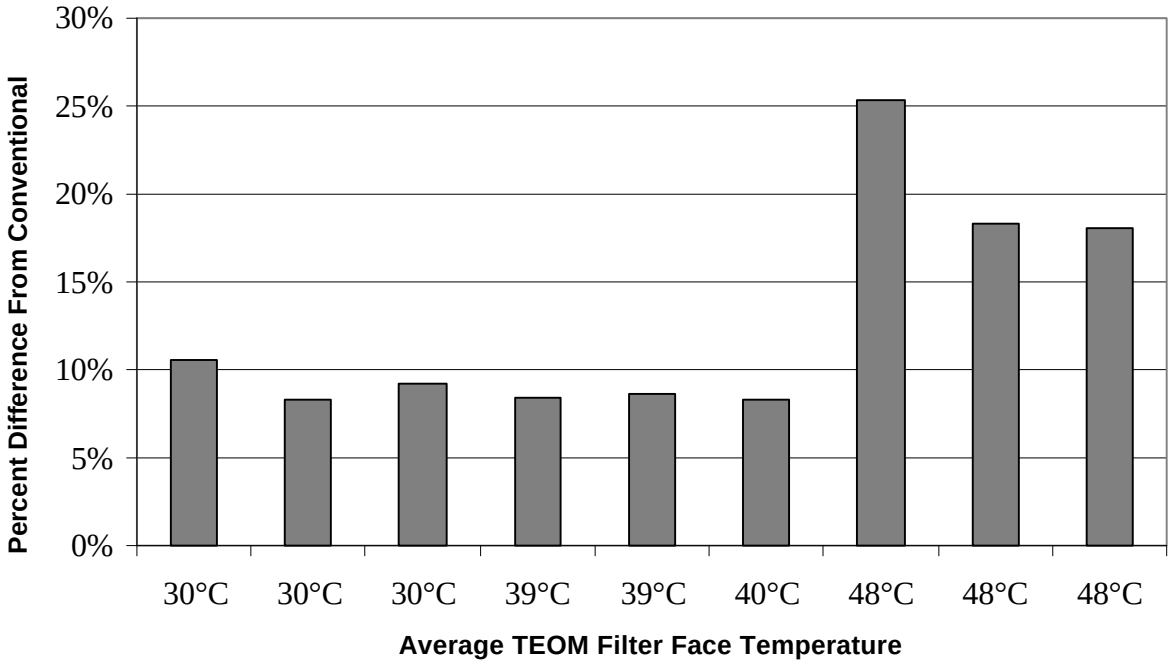

Figure 25: Error data for varying TEOM sample tube temperatures.
The greatest error occurred at 50°C.

For the Navistar, the best measured TEOM to conventional PM agreement sampling temperature was 35°C. This was also the closest applied TEOM temperature to the conventional PM temperature. This trend continues in the Cummins data. For the best agreement with conventional PM results, the TEOM temperature set point was close to the conventional PM filter temperature. This ideal temperature can be adjusted in the test rig by varying the dilution ratio of the dilution tunel (see section 3.1.1.2).

Temperature also affects real-time TEOM data. The Cummins data were chosen to evaluate real-time results due to the consistent trend of the data. Tests 2, 6 and 9 were chosen to represent 30 °C, 40 °C and 50 °C set points on least error criteria. FTP data shows that as TEOM temperature increased, amplitude of the response decreased, both positive and negative. Figure 26 shows a section of the FTP cycle to illistrate this trend. However, as TEOM temperature increased, the ratio of the total positive mass collected to negative mass collected increased, as shown in table 12. The 50 °C set point yielded the least collection of negative mass per positive mass collection. The 50 °C set point also yielded a 11% lower total collection, whereas the 30 °C and 40 °C set points yielded total collection mass less than 1% from each other. Figure 27 illustrates this real-time total collection data.

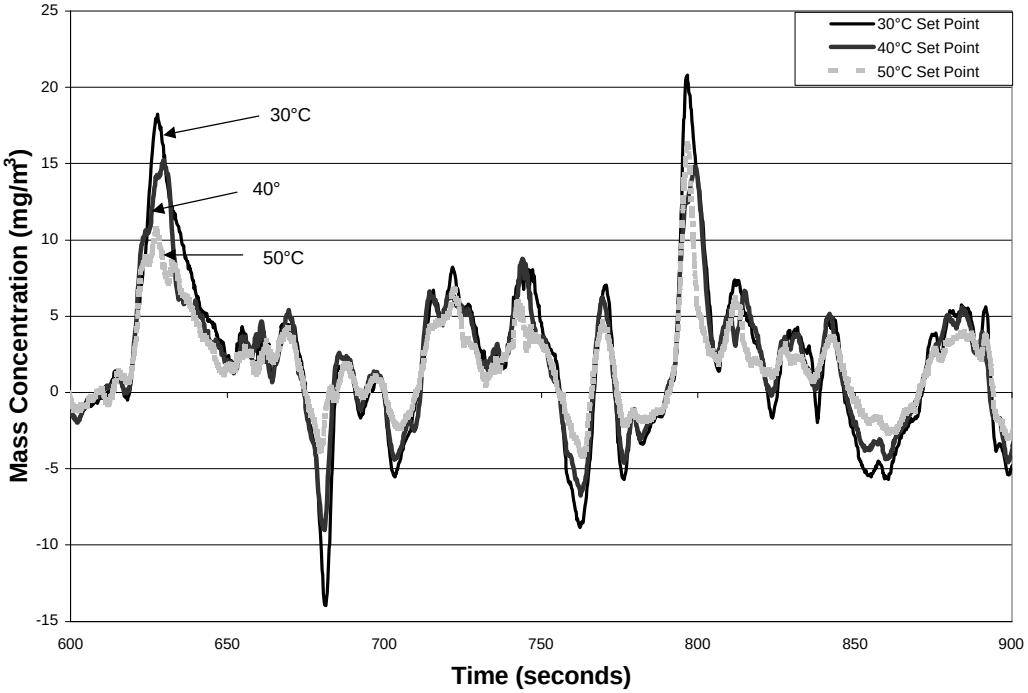

Figure 26: A section of the FTP illustrating that increased temperature decreased TEOM real-time data amplitude.

Table 12: Real-time positive/negative collection evaluation for varying air temperature.

TEOM Temperature Set Point	30°C	40°C	50°C
Positive Collected Mass (micrograms)	120.83	107.96	85.43
Negative Collected Mass (micrograms)	49.61	38.47	23.48
Positive/Negative Ratio	2.44	2.81	3.64

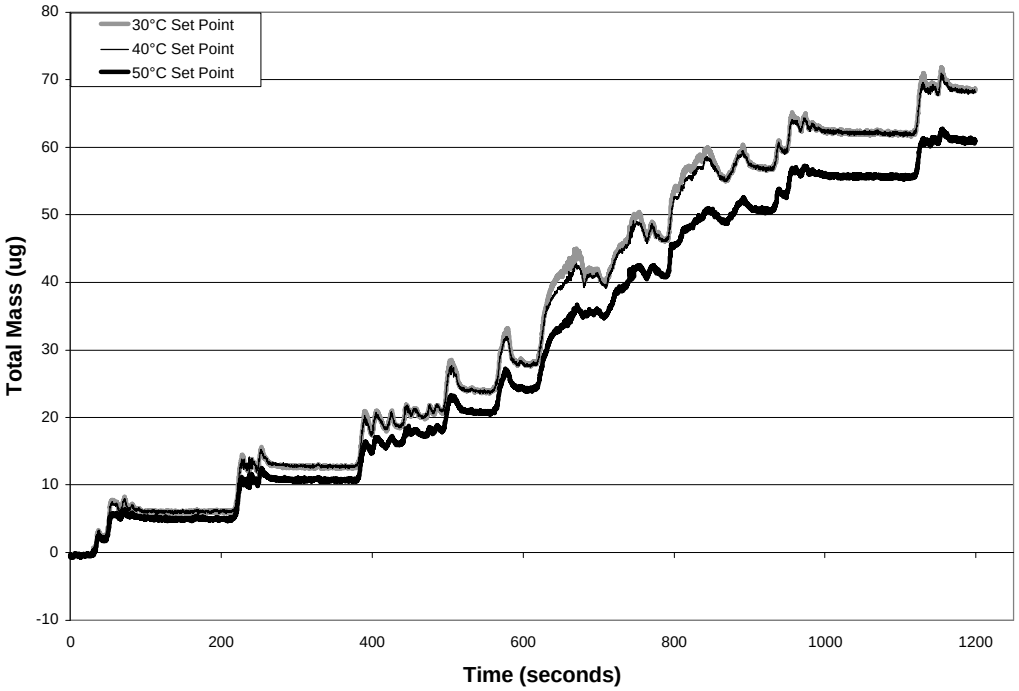

Figure 27: TEOM sampling temperature effects on total mass. The 50 °C set point yielded an undercollection compared to the other two set points.

To illustrate the repeatability of the data, figures 28 and 29 display mass rate and total mass respectively for two sequential tests at the same TEOM temperature and flow set points. The sequential experiments graphed were tests 2 and 3 from the Cummins temperature study. Note that both real-time mass rate and total mass traces follow closely to each other. The real-time mass rate traces do deviate as could be expected due to variations in engine output from test to test.

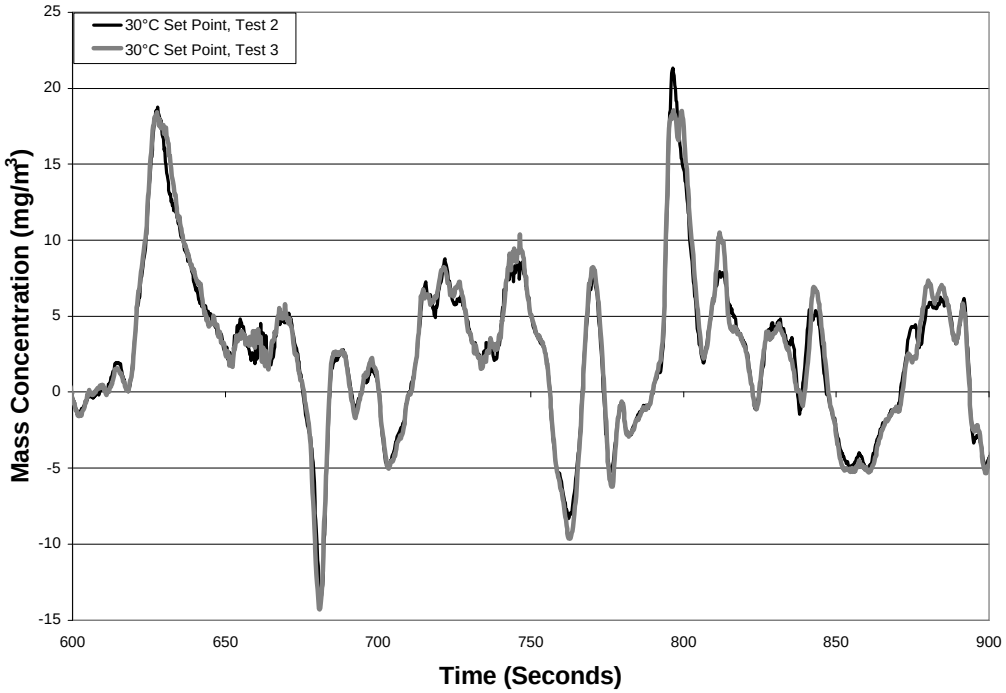

Figure 28: A section of the FTP illustrating the repeatability of the real-time results. The deviation of the two traces could be from variation of engine output.

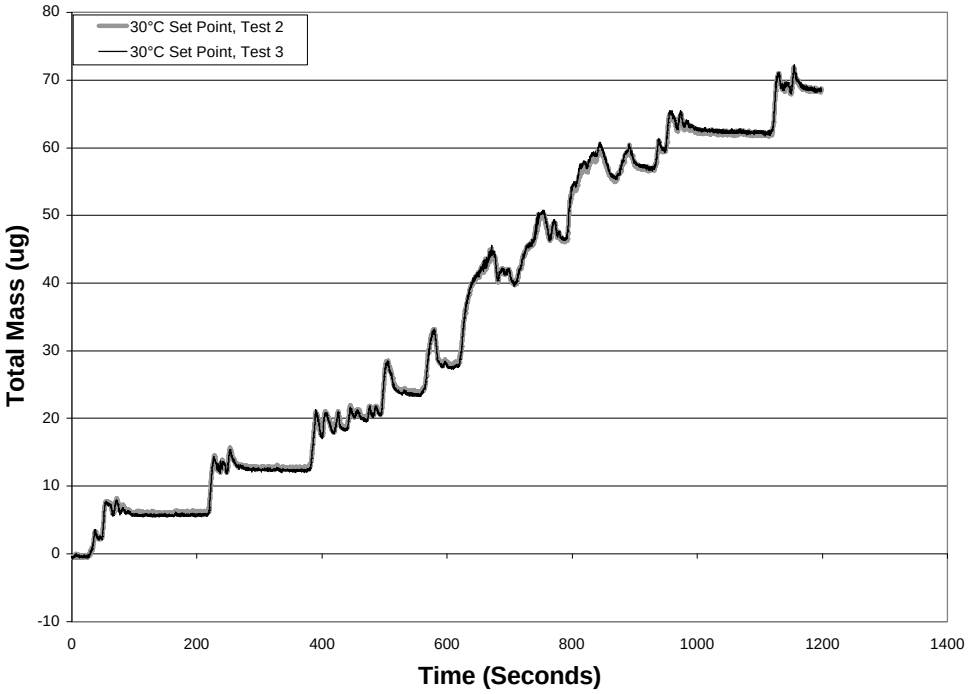

Figure 29: The accumulated mass as measured by the TEOM, illustrating test to test repeatability.

In closing, due to the better conventional PM agreement and medium positive/negative collection ratio, the 40°C set point was chosen to perform the flow effects investigation described in the next section.

5.2 Flow Effects

Using the 40°C set point, flow was varied from 1 to 4 lpm. The EPA range for filter face flux is 0.792 liters per cm^2-minute to 2.638 liters per cm^2-minute. The TEOM effective filter face was approximately 1.23 cm in diameter, giving an EPA allowable TEOM sample rate of 0.97 lpm to 3.24 lpm. The conventional PM filter system had an effective filter face diameter of 6.2 cm. All conventional PM samples were taken at approximately five SCFM, or 141 lpm, yielding 4.69 liters per cm^2-minute. Sampling at four lpm is outside of the EPA allowable range, however investigation could yield interesting results. The tests were conducted on the Cummins 10.8 liter DI diesel engine. The use of this engine was mandatory due to the precedence of other engine programs at the EERC. The engine was operated through a FTP cycle to bring the engine and tunnel to operating temperature before data were taken. Eight FTP cycles were run back to back with a nominal engine off time of 10 minutes between tests. When the TEOM filter was changed, an FTP was run to condition the filter in an attempt to eliminate the variable of filter efficiency. These conditioning FTPs were not included in the analysis of the data. However, sampling at 4 lpm caused a filter loading high enough to restrict multiple tests per TEOM filter, so a new filter was used for each test. The COV% for the eight tests of conventional PM flow normalized data was 3.2%, proving data viability. The average relative humidity of the ambient air for the duration of the test series was 25%. Table 13 and figure 30 show data results for the flow tests. As a general trend, as flow increased, so did the percent difference. Although the exception is at 2 lpm, where there was not as a significant increase.

Table 13: Error variation with TEOM sample flow rate.

Test #	TEOM Sample Flow Rate (lpm)	Conventional PM Concentration (mg/m^3)	TEOM Concentration (mg/m^3)	Percent Difference From Conventional
1	1.00	1.20	1.09	9.7%
2	1.00	1.25	1.13	10.2%
3	2.00	1.29	1.15	10.7%
4	2.00	1.25	1.12	10.1%
5	3.00	1.17	1.01	14.4%
6	3.00	1.25	1.10	12.1%
7	4.00	1.29	1.05	18.3%
8	4.00	1.27	0.97	23.4%

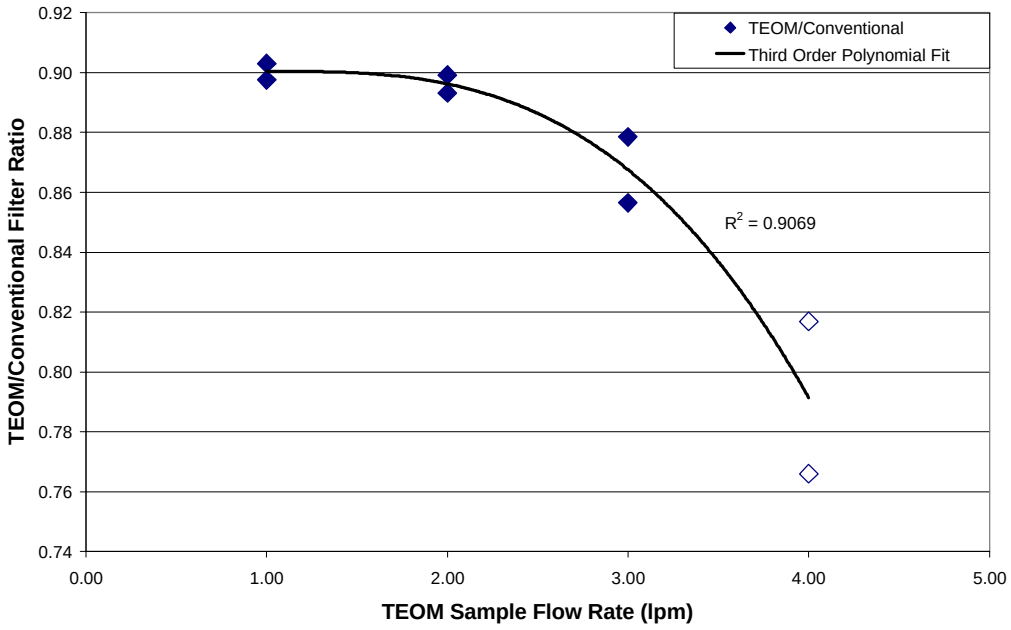

Figure 30: TEOM/conventional PM ratio as TEOM sample flow rate was varied on the Cummins engine. The hollow data points represent tests that required a new TEOM filter, solid data points represent test taken with a used TEOM filter.

Note that tests five and six have the same TEOM settings as tests four, five, and six in the Cummins section of temperature effects, namely 40°C sample path temperature and three lpm sample rate. However, the tests in the temperature effects section resulted in a lower error value. This was due to a cooler conventional PM air temperature during the flow effect test series. The cooler conventional PM temperature was a result of cooler ambient conditions. As TEOM sample flow rate increased, TEOM values increasingly deviate from conventional PM results. Results from tests seven and eight would have been closer to conventional PM values if new filters were not required for each test.

As with temperature, flow also affected real-time data. Tests one, four, six, and seven were chosen to represent one, two, three, and four lpm set points on least error criteria. Figure 31 and table 14 display real time data results.

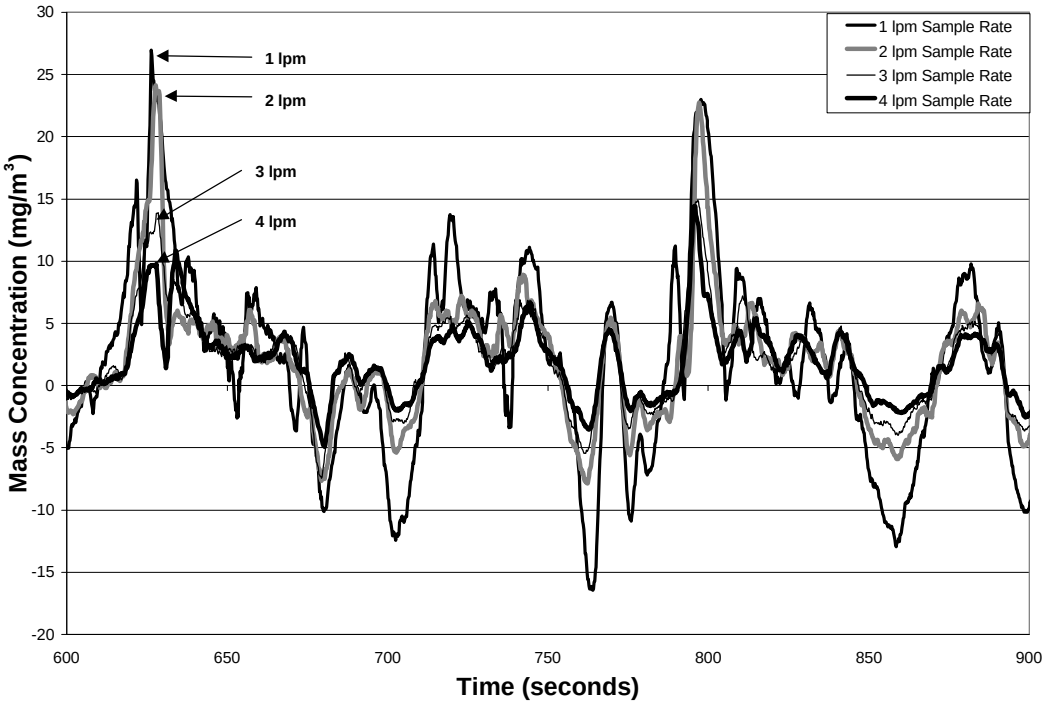

Figure 31: A section of the FTP illustrating increased flow decreased TEOM real-time data amplitude.

Table 14: Real-time positive/negative collection evaluation for varying flow rate.

TEOM Sample Flow Rate (lpm)	1.00	2.00	3.00	4.00
Positive Collected Mass (micrograms)	55.62	77.15	99.04	111.24
Negative Collected Mass (micrograms)	33.10	31.49	32.05	25.57
Positive/Negative Ratio	1.68	2.45	3.09	4.35

FTP data show that as TEOM sample rate increased, amplitude of the response, both positive and negative decreased. However, as TEOM sample rate increased, the ratio of the total positive mass collected to negative mass collected increased. The four lpm yielded the least collection of negative mass per positive mass collection. The 99% confidence value of the conventional PM concentration for the 17 tests (temperature and flow tests) recorded on the Cummins engine was ±1.7%, or 1.24 ±0.021 mg/m^3. The 99% confidence of the TEOM measurements for the Cummins data set was ±4.3%, or 1.08 ±0.047 mg/m^3. Note an improvement in confidence level between the Navistar and the Cummins. The data suggests that this improvement was caused by disregarding the tests with new filters.

5.3 Sample Location Effects

The tests were conducted on the Cummins 10.8 liter DI diesel engine. The engine was operated through a FTP cycle to bring the engine and tunnel to operating temperature before data were taken. Three FTP cycles were run back to back with a nominal engine off time of 10 minutes between tests. The COV% of the conventional PM flow normalized data was 1.9%, demonstrating data viability. A new TX40 filter was installed in the TEOM before the test series began. The average relative humidity of the ambient air for the duration of the test series was 25%. Results shown in table 15 are from sampling at the secondary tunnel.

The third test in the series yielded the lowest error value in the Cummins test battery. However, when compared to the Cummins, 40°C, three lpm data taken during temperature tests, the improvement was less than a percent, as shown in table 15. This improvement was well within the 99% confidence range of ±4.3%, and thus qualifies this improvement as negligible. Moving the sampling location did affect the real-time data. The real-time data were smoother possibly due to pressure dampening from the secondary tunnel dead volume, as shown in figure 32.

Table 15: Results of sampling from the secondary dilution tunnel.

Test Number	TEOM Flow Set Point (lpm)	TEOM Temperature Set Point (°C)	Conventional PM Concentration (mg/m^3)	TEOM Concentration (mg/m^3)	Percent Difference From Conventional
1	3	40	1.59	1.31	17.9%
2	3	40	1.55	1.42	8.8%
3	3	40	1.56	1.44	7.7%

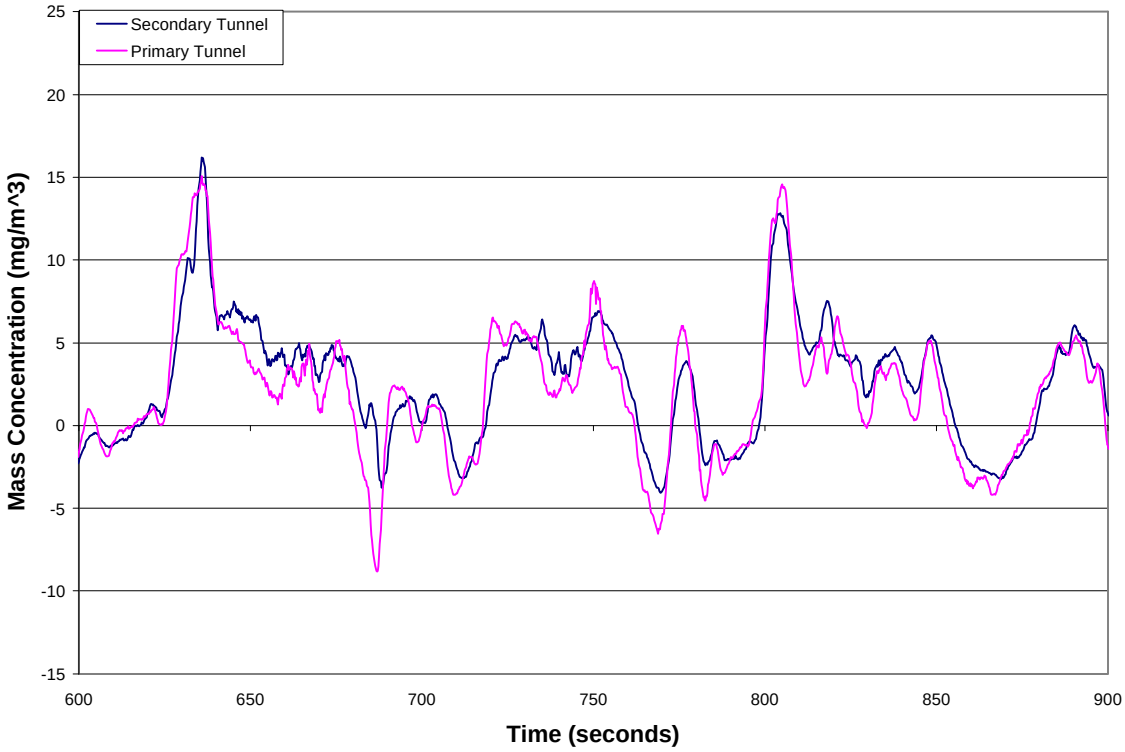

Figure 32: A section of the FTP illustrating sample location effects on real-time TEOM data.

Table 16: Positive/negative collection evaluation for secondary tunnel sampling.

Location	Secondary Tunnel, Test 2	Secondary Tunnel, Test 3	Primary Tunnel, Test 5	Primary Tunnel, Test 6
Positive Collected Mass (micrograms)	108.72	111.86	104.96	106.92
Negative Collected Mass (micrograms)	21.06	23.50	36.85	36.66
Positive/Negative Ratio	5.16	4.76	2.85	2.92

Moving the sample location also improved the positive mass collection, as well as decreasing the negative mass collection, as shown in table 16. Other cycles showed improvement due to sample location and temperature changes also.

When the WVU FTP 75 cycle was applied to the Navistar 7.3 liter, slight improvements were made to the conventional PM/TEOM agreement, as catalogued in table 17. Three systems were tested with the WVU FTP 75 cycle. System 1 was a conventional exhaust routing with all exhaust routed to the dilution tunnel. In system 2, flow was split in approximately one-half to create a base line for investigating catalyst effects and routed into the dilution tunnel for a separate project. In system 3, the

split flow system was used to evaluate an oxidation catalyst. The data in table 17 illustrates the variability in TEOM collection when the test system was varied. The best agreement between TEOM and conventional PM for this cycle was 15.1% difference when sampled from the secondary tunnel. In comparison, the best heavy-duty FTP cycle agreement for the secondary tunnel was 7.7% difference.

Table 17: WVU FTP 75 comparison of sampling modification results shows a 10.6% average improvement

Sampled from the Secondary Tunnel at 40°C and 3 lpm.	Conventional PM Concentration (mg/m^3)	TEOM Concentration (mg/m^3)	Percent Difference From Conventional
System 1	1.25	0.99	21.0%
System 2	1.14	0.46	59.5%
System 3	0.51	0.41	19.1%
System 1	1.10	0.93	15.1%
System 2	0.79	0.57	28.0%
Sampled from the Primary Tunnel at 50°C and 2 lpm.	Conventional PM Concentration (mg/m^3)	TEOM Concentration (mg/m^3)	Percent Difference From Conventional
System 1	0.56	0.44	22.1%
System 2	0.92	0.36	61.2%
System 3	1.31	0.88	32.6%
System 1	0.84	0.50	40.7%
System 2	1.42	0.86	39.0%

5.4 Filter Conditioning

Five types of tests were performed to investigate the effect of filter pre-conditioning on start up after filter replacement. Multiple tests were performed for each type of conditioning, but only the worst case results are shown in figure 33. The objective was to find the maximum time need to bring a filter to a stable state.

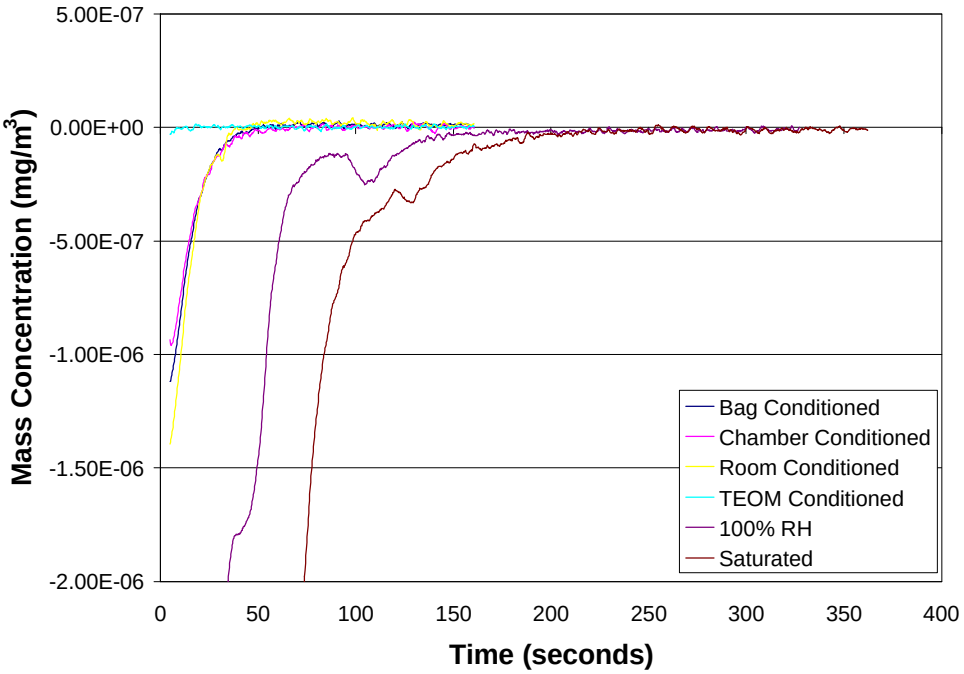

Figure 33: Mass concentration response due to different filter conditioning.

The TEOM was set to sample at 50°C and 2 lpm during all tests except 100% RH tests. In 100% RH tests, results from 50°C, 2 lpm settings were compared to 40°C, 3 lpm settings, worst case is shown, a test from 40°C, 3 lpm. In the worst case, filter saturation, the TEOM was ready to sample by 350 seconds or approximately 6 minutes. Under normal conditioning criteria, such as storing the filters in the R&P bag, the TEOM was ready to sample within 75 seconds. It is uncertain what caused dips in the data from the 100% RH and Saturated tests.

5.5 Effect of Filter Type

The tests were conducted on the Cummins 10.8 liter DI diesel engine. The engine was run through an FTP cycle to bring the engine and tunnel to operating temperature before data were taken. Four FTP cycles were run back to back with a nominal heat soak time of 10 minutes between tests. The COV% of the conventional PM flow normalized data was 1.2%, proving data viability. The average relative humidity of the ambient air for the duration of the test series was 27%. The TEOM temperatures were set to 40°C while flow rate was set to 3 lpm.

Table 18: Results from using T60A20 filters in the TEOM.

Conventional PM Average Temperature (°C)	TEOM Temperature Set Point (°C)	Conventional PM Concentration (mg/m^3)	TEOM Concentration (mg/m^3)	Percent Difference From Conventional
30	40	1.21	0.78	35.97%
34	40	1.23	0.97	21.37%
35	40	1.20	1.00	16.33%
36	40	1.20	1.03	14.35%

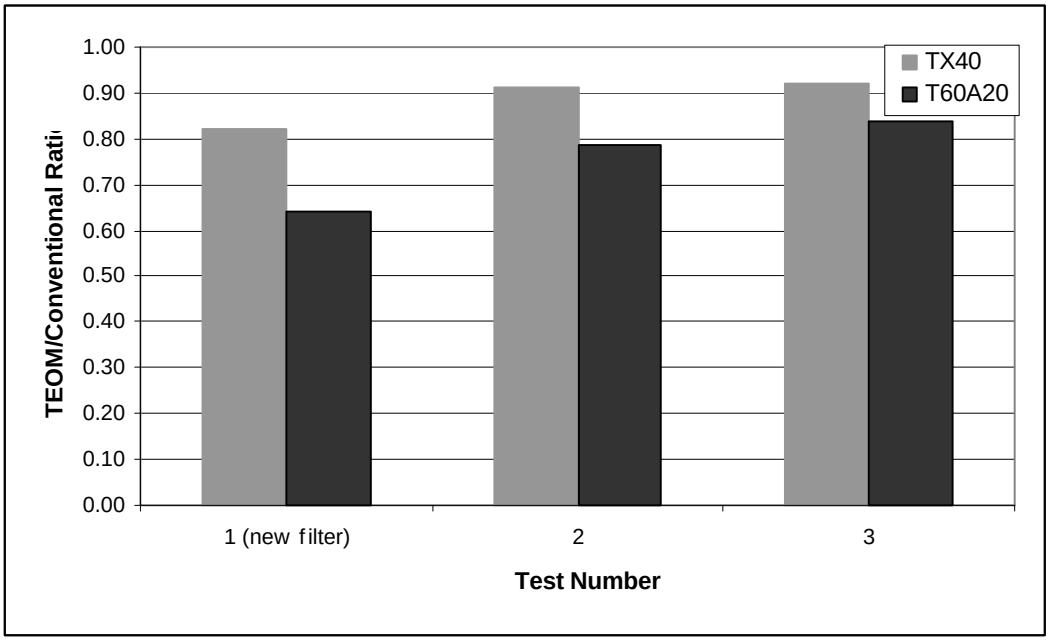

Figure 34: Error showing the initial collection efficiency of TX40 and T60A20 filter media types.

Collection efficiency was lower for the T60A20 than the TX40, as communicated in table 18 and figure 34. The medium used for conventional PM capture was T60A20. From these filter media tests, the difference in previous comparisons between TEOM and conventional measurements could even be more exaggerated when filter media are equivalent.

6 Real-time Observations

Real-time data were graphed with data from other real-time analyzers to search for relationships or characteristics of PM. Data were time shifted based on the results of the correlation program. Figure 35 shows the results of the program, were the peaks in the graph represent the best time shift (delay) each emission. The correlation coefficient equation is listed in section 4.6.

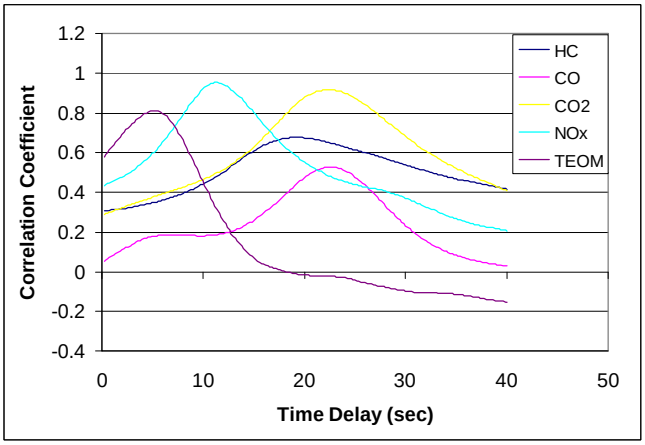

Figure 35: Results from the cross correlation program, where peaks in data represent best estimated time shift. TEOM data were the least delayed, possibly due to the fast response of the instrument and shorter sample length. Validation of the time shifting program can be found in Appendix C.

For ease of reading and comparison, chart data are normalized by dividing the real-time values by the average, creating average normalized data.

No strong correlations, determined by a coefficient of determination (r^2) close to one, were found between TEOM and HC, CO_2, and NO_X for the FTP cycle. In figure 36, an increase in TEOM value seemingly corresponds to increased in HC. However, figure 37 shows no significant correlations are evident. The trend in figure 36 could be due to turbocharger lag or possibly an over fueling condition from transient maneuvers. Figure 38 shows average normalized CO and TEOM real-time data for the FTP cycle. The CO data tends to follow the TEOM data with exception to the zones of high speed in combination with varying or low load conditions. A slight (r^2=0.49) linear relationship with CO was found. This supports work done by Jarret et al. [16]. The real-time TEOM data tended to correlate best with CO during regions of high torque in figure 39. Low torque, high-speed regions did not yield a linear relationship, but clock-wise forming loops. The larger loops relate to the zones of high speed in combination with low load conditions. An example of these loading conditions is from 600 to 900 seconds during the FTP cycle. In the author's experience with electronic engine controls, these larger loops could be formed from inconstancies in fuel control during low air mass conditions. The varying fuel mass could be due to the low duty cycle of injectors, where the injection error is a

larger fraction of the total amount of fuel delivered. A trend between TEOM and CO as well as HC was expected. Relationships were CO might correlate with soot and HC with the SOF. However, soot would correlate better due its closer relationship with transient fueling, hence a better correlation with CO. In figure 40, normalized CO_2 and TEOM real-time data for the FTP cycle are plotted. The amplitude and duration of the TEOM spikes do not correlate with the CO_2 spikes thought the cycle. Average normalized CO_2 versus TEOM real-time data is shown in figure 41. This figure shows that there is a slight upward trend between CO_2 and real-time TEOM data with a coefficient of determination of 0.53. As with CO, CO_2 had a clockwise forming loop relationship with TEOM data. Figure 42 illustrates average normalized time derivative of CO_2 and TEOM real time data for the FTP cycle. Additional time shifting brought about a correlation, which could correspond to a turbocharger lag. Figure 43 illustrates the relationship of average normalized time derivative of CO_2 verses TEOM real-time data. Figures 44 and 45 illustrate the relationship that was found between NO_x and TEOM real-time data. The amplitude and duration of the TEOM spikes do not correlate with the NO_x spikes thought the cycle. Note the similarities between figure 41 and 45 as NO_x is closely related to CO_2 on an energy specific basis. Torque and TEOM, shown in figures 46 and 47, seem to folow each other with exception to the zones of high speed in combination with low load conditions. A second order polynomial correlation between torque and real-time TEOM data was found. The areas of high speed in combination with varying or low load conditions tend to give a weaker relationship. For example, around the time of 230 seconds and from 600 to 900 seconds (see Figure 2 for the speed and load points during an FTP).

Inconsistent TEOM results were found when comparing FTP data to WVU FTP 75 data. Trends found in FTP tests were not always found in WVU FTP 75. The exception to this was CO, forming an upward trend in counterclockwise loops, as illustrated in figure 48. Figure 49 shows the linear relationship of NO_X and TEOM with a coefficient of determination of 0.57. NO_X data displayed a relationship with TEOM for the WVU FTP 75 that was not as apparent with the FTP. It appears that two modes of operation are shown. A weak second order polynomial correlation between torque and real-time TEOM data was found of the FTP cycle. The correlation did not prove to be apparent in the WVU FTP 75 cycle, as shown in figure 50.

Trends in the CBD seemed to be different yet again, however, it should be noted that the CBD cycle is a simple, repetitive test, where the same trend will repeat, giving a false “correlation”. See figure 12 for the vehicle speed during a CBD. Figures 51, 52 and 53 display the relationship between TEOM and CO, NOx and axle power respectively. A correlation between CO, NOx and axle power and real-time TEOM data were evident.

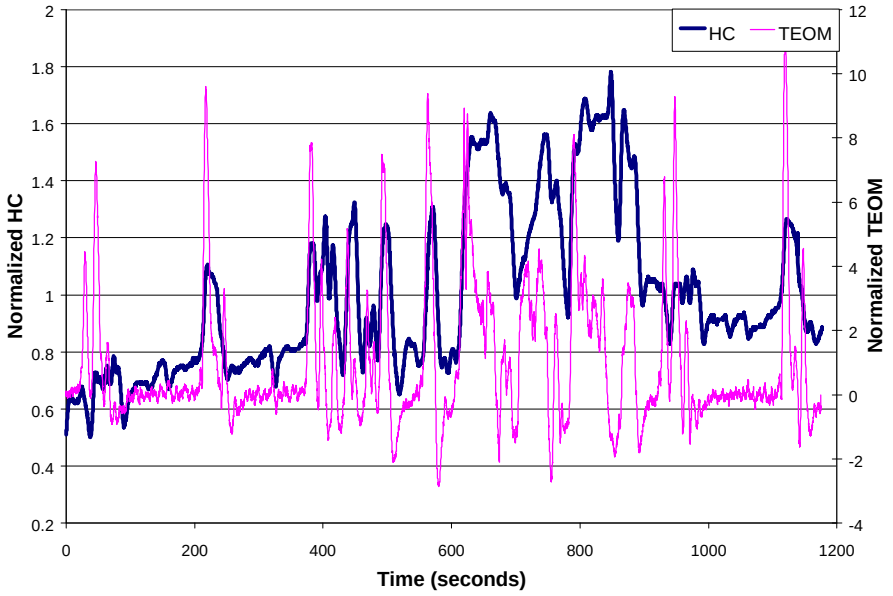

Figure 36: Average normalized HC and TEOM real-time data for the FTP cycle. The amplitude and duration of the TEOM spikes do not correlate with the HC spikes thought the cycle.

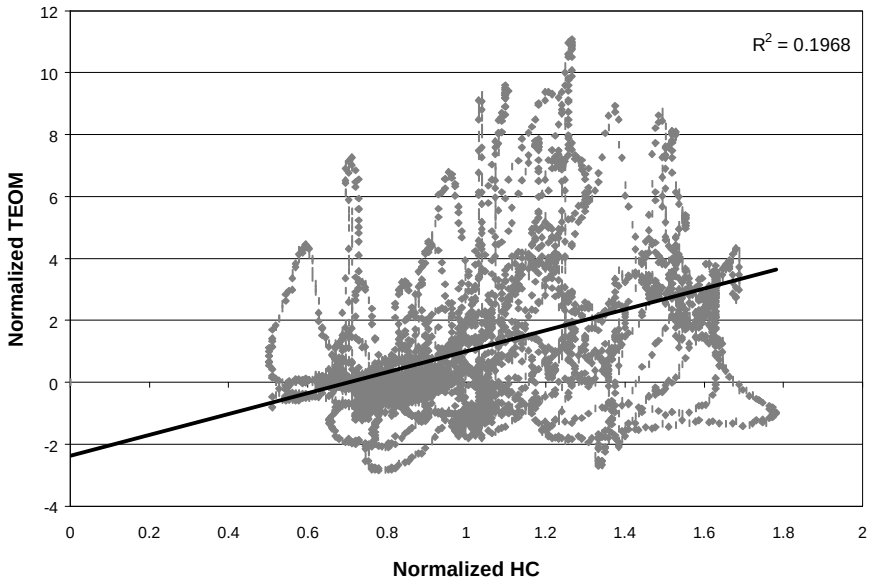

Figure 37: Average normalized HC versus TEOM real-time data for the FTP cycle. There was not a correlation between HC and real-time TEOM data.

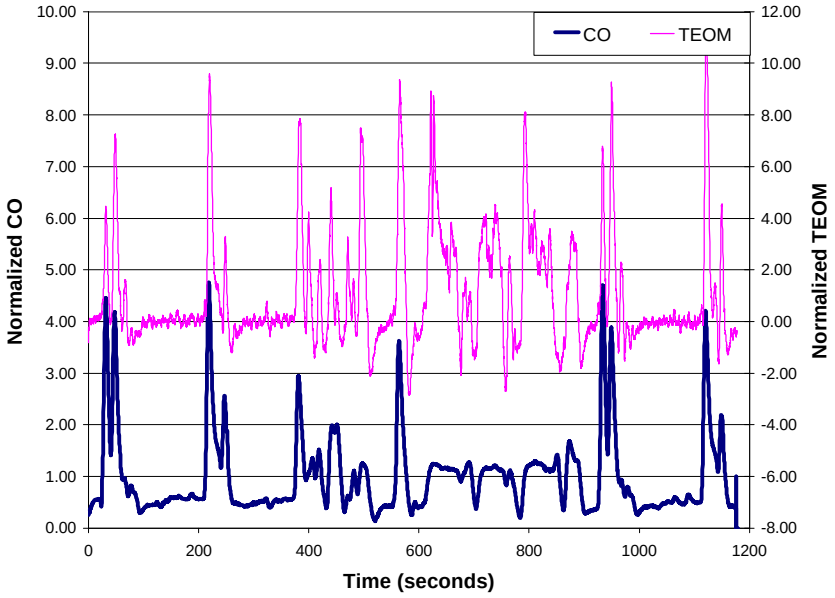

Figure 38: Average normalized CO and TEOM real-time data for the FTP cycle. The CO data tends to follow the TEOM data with exception to the zones of high speed in combination with varying or low load conditions.

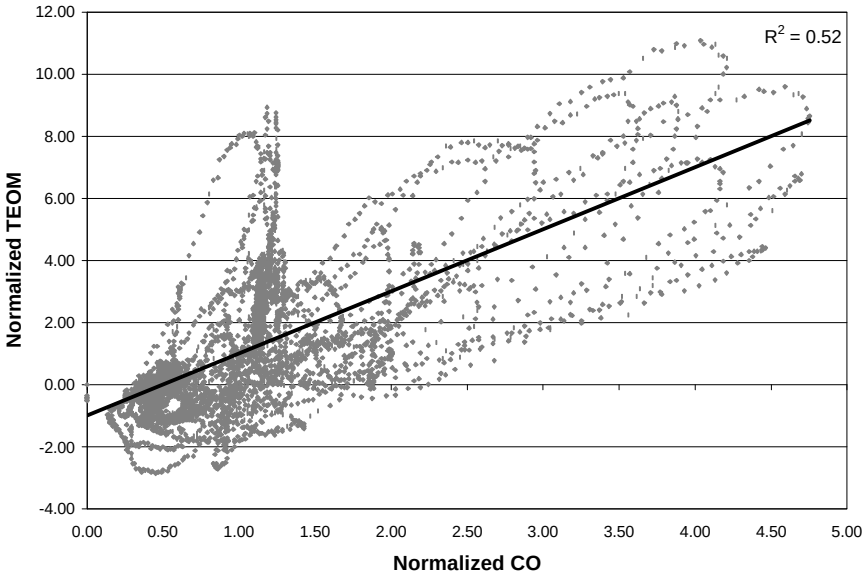

Figure 39: Average normalized CO versus TEOM real-time data for the FTP cycle. A weak linear correlation between CO and real-time TEOM data were shown. This does support the conclusions reached by Clark [16]. The larger loops relate to the zones of high speed in combination with low load conditions. For example, around the time of 230 seconds and from 600 to 900 seconds (see Figure 2 for the speed and load point during an FTP).

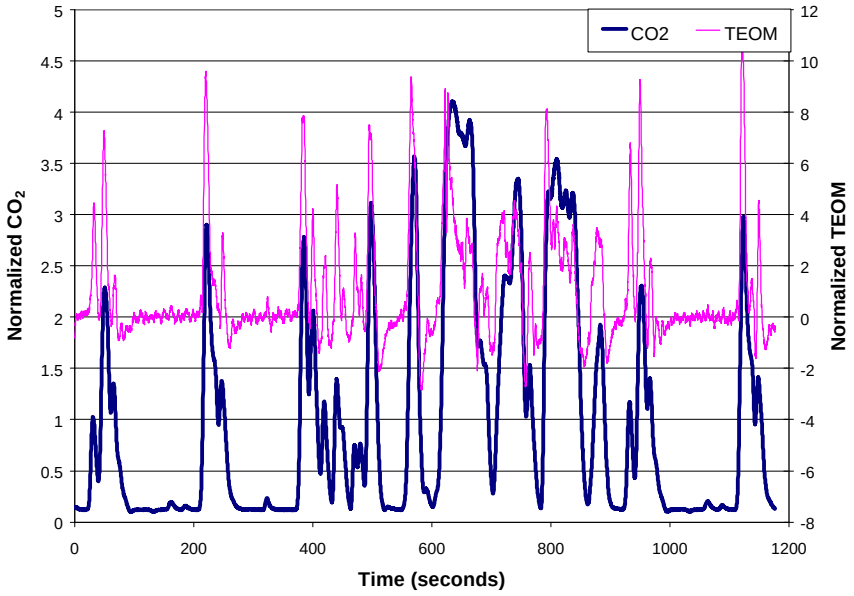

Figure 40: Average normalized CO_2 and TEOM real-time data for the FTP cycle. The amplitude and duration of the TEOM spikes do not correlate with the CO_2 spikes thought the cycle.

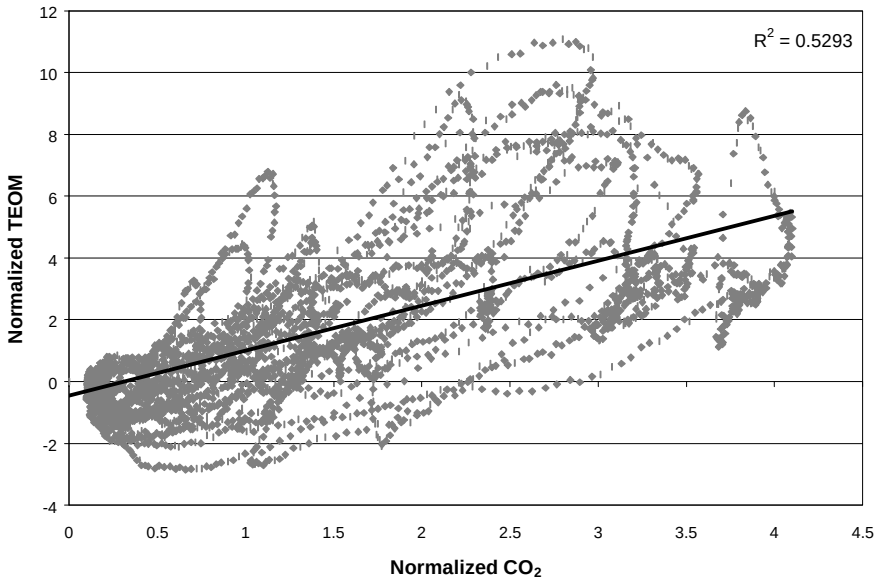

Figure 41: Average normalized CO_2 versus TEOM real-time data for the FTP cycle. This figure shows that there was a slight upward trend between CO_2 and real-time TEOM data.

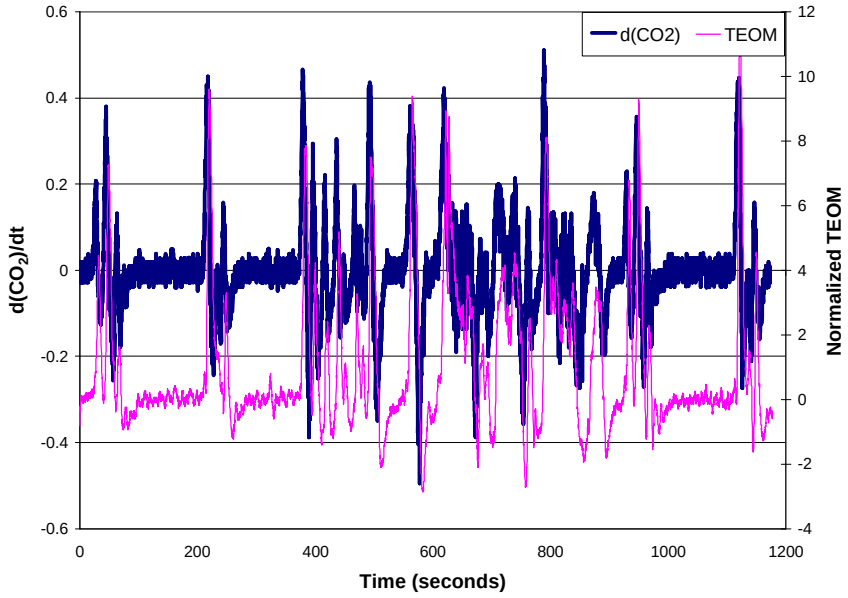

Figure 42: Average normalized time derivative of CO_2 and TEOM real time data for the FTP cycle. Additional time shifting brought about a correlation, which could correspond to turbocharger lag.

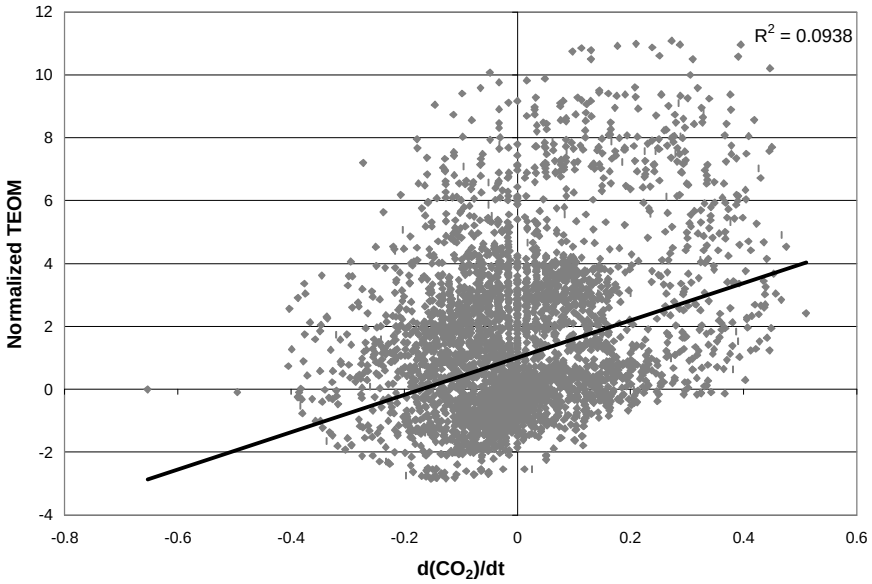

Figure 43: Average normalized time derivative of CO_2 versus TEOM real-time data for the FTP cycle.

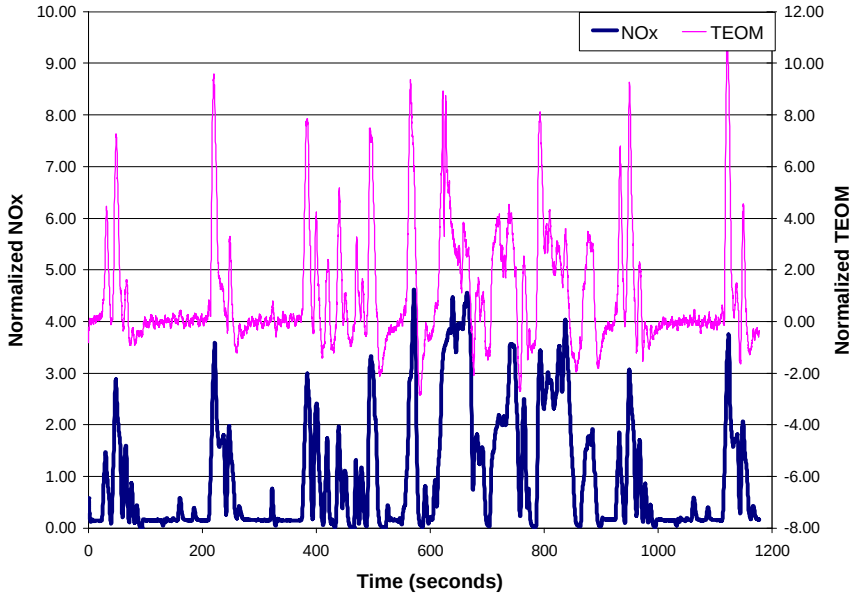

Figure 44: Average normalized NO_x and TEOM real-time data for the FTP cycle. The amplitude and duration of the TEOM spikes do not correlate with the NO_x spikes thought the cycle.

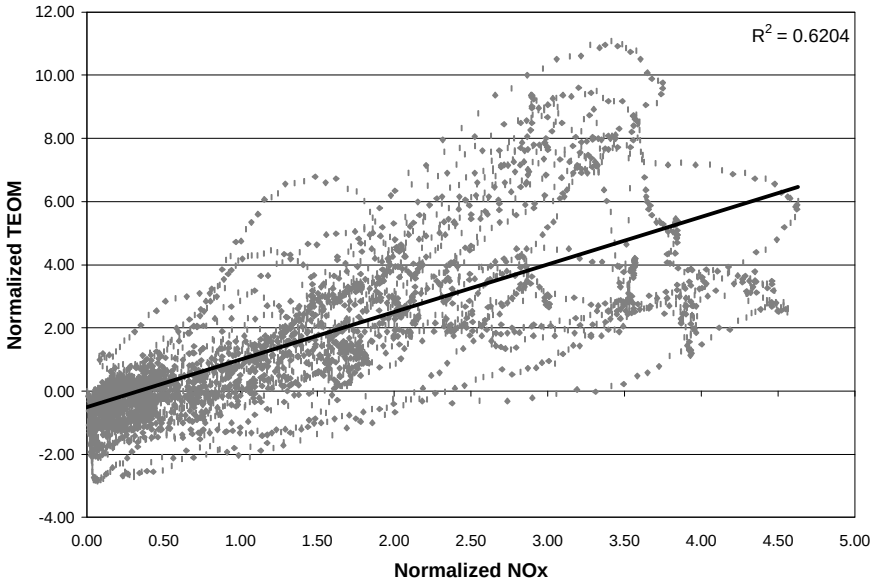

Figure 45: Average normalized NO_x versus TEOM real-time data for the FTP cycle. There was a slight upward trend between NO_x and real-time TEOM data.

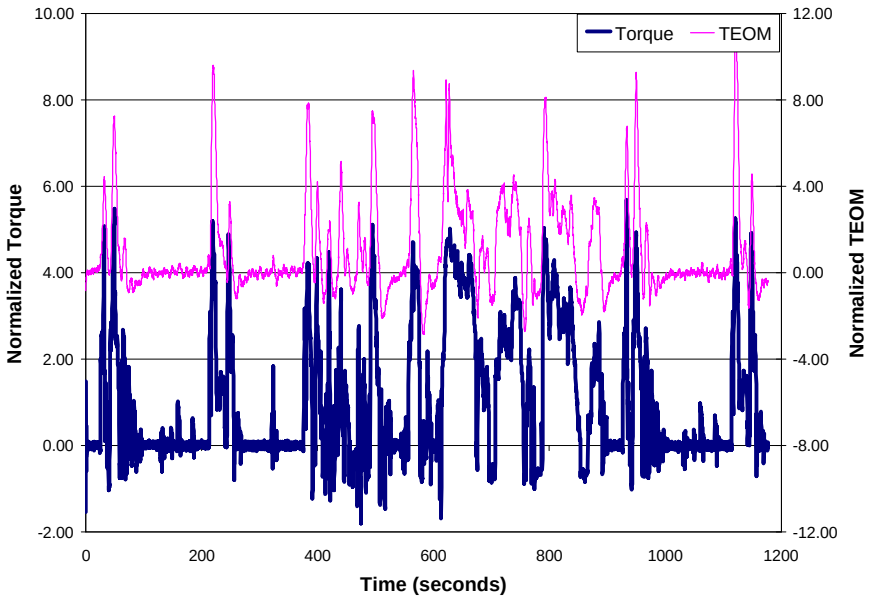

Figure 46: Average normalized torque and TEOM real-time data for the FTP cycle. The torque data tends to follow the TEOM data with exception to the zones of high speed in combination with low load conditions.

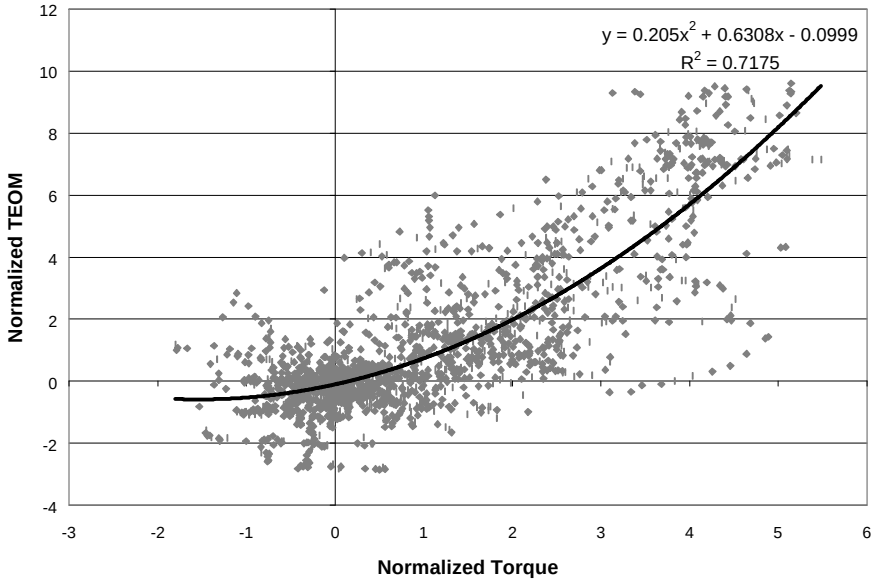

Figure 47: Average normalized torque versus TEOM real-time data for the FTP cycle. This figure shows that there was a weak second order polynomial correlation between torque and real-time TEOM data. The areas of high speed in combination with varying or low load conditions tend to give a weaker relationship. For example, around the time of 230 seconds and from 600 to 900 seconds (see Figure 2 for the speed and load points during an FTP).

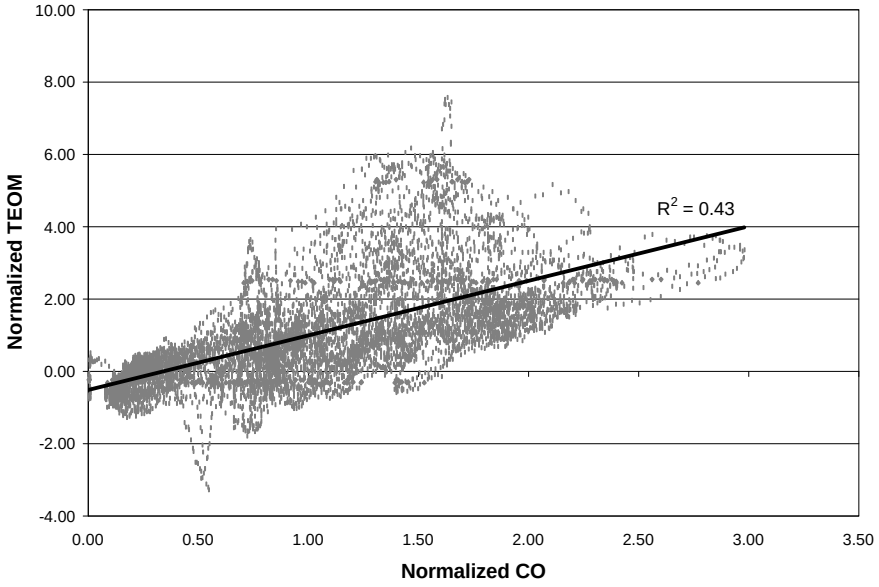

Figure 48: Average normalized CO versus TEOM real-time data for the WVU FTP 75 cycle. This figure shows that there was a weak linear correlation between CO and real-time TEOM data.

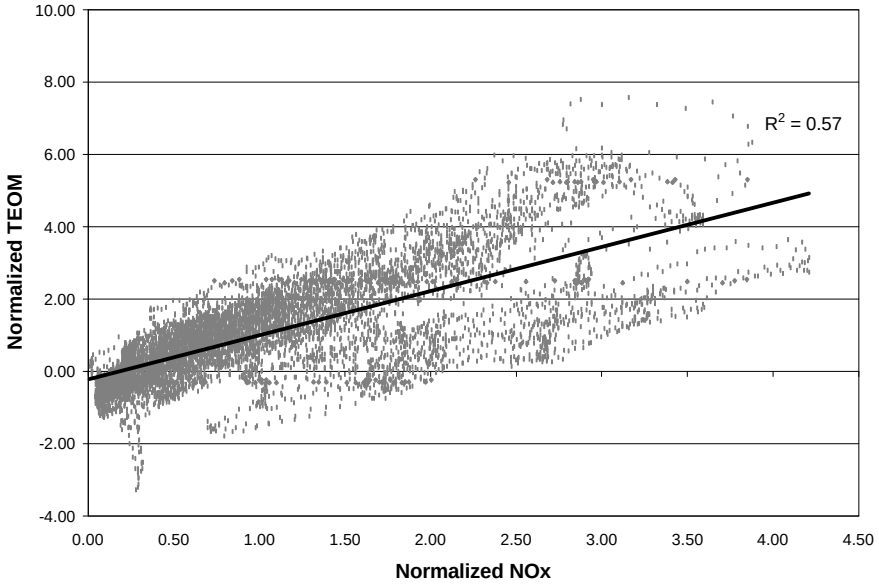

Figure 49: Average normalized NOx versus TEOM real-time data for the WVU FTP 75 cycle. A weak linear correlation between NOx and real-time TEOM data were shown. It appears that two modes of operation are shown here.

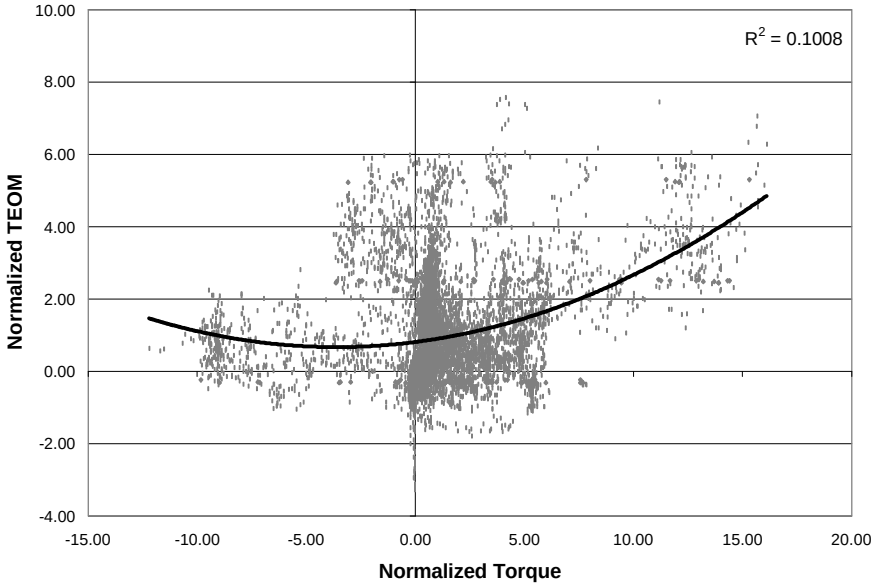

Figure 50: Average normalized torque versus TEOM real-time data for the WVU FTP 75 cycle. The second order polynomial correlation found with the FTP cycle did not prove to exist with the FTP75.

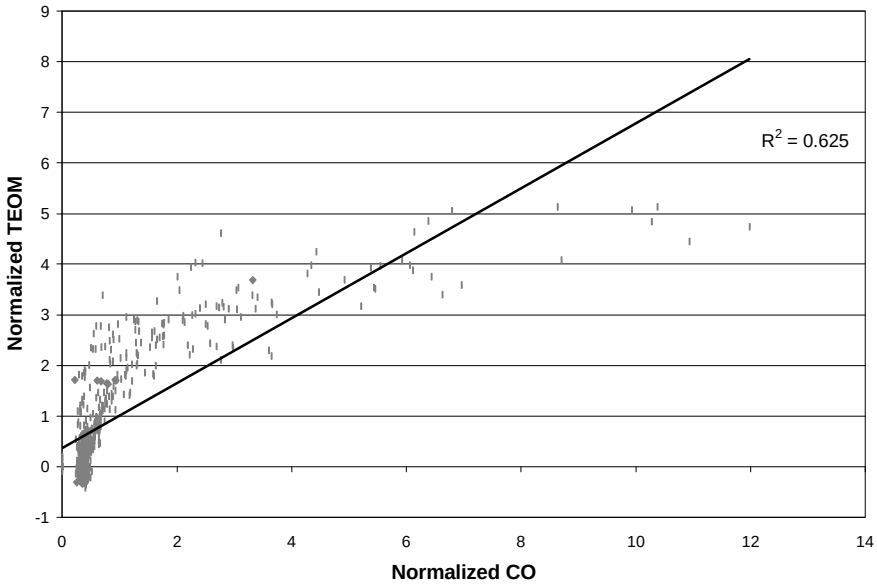

Figure 51: Average normalized CO versus TEOM real-time data for the CBD cycle. A correlation between CO and real-time TEOM data were evident. See figure 12 for the vehicle speed during a CBD.

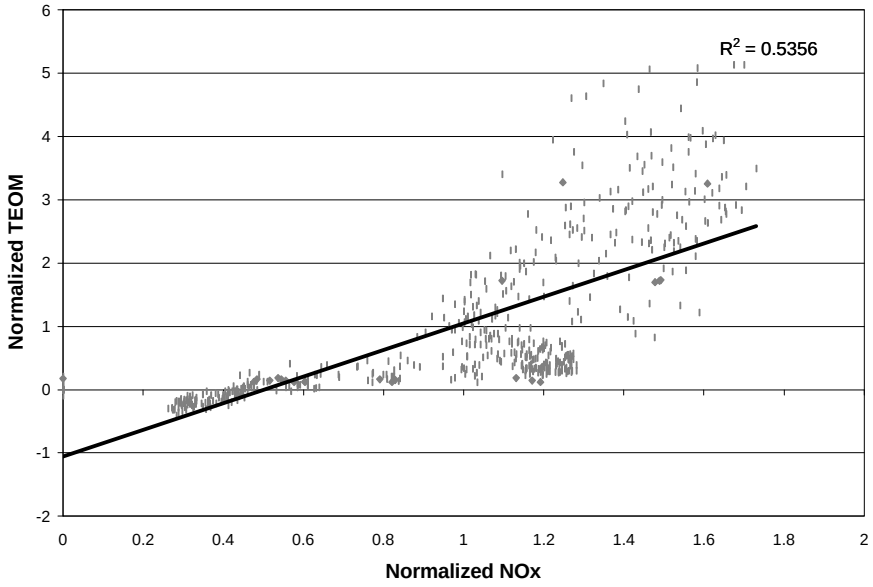

Figure 52: Average normalized NO_x versus TEOM real-time data for the CBD cycle. A correlation seems to exist, however, the CBD cycle was a repetitive cycle. A trend is likely to repeat, looking as if there is a good correlation.

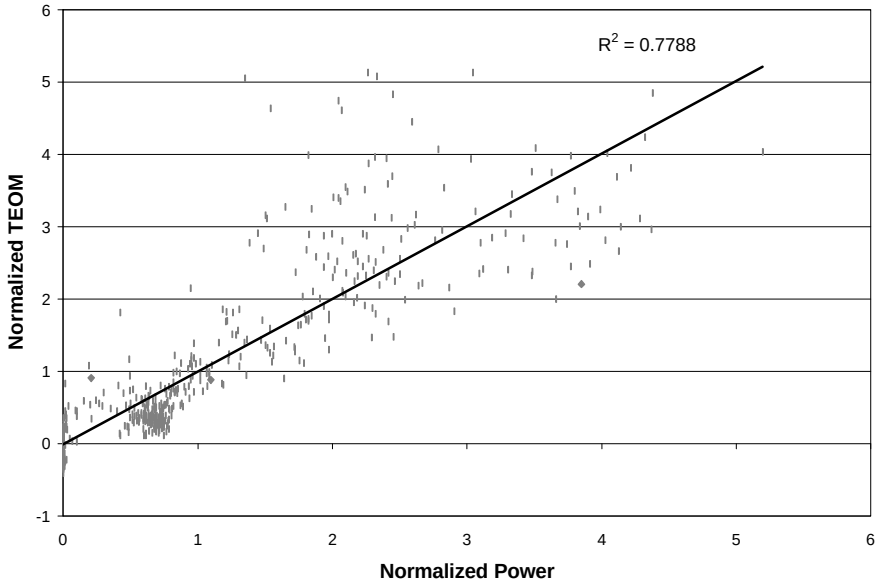

Figure 53: Average normalized axial power versus TEOM real-time data for the CBD cycle. Again, a trend will recur with this repetitive cycle.

7 Conclusions

A TEOM series 1105 diesel particulate mass monitor was operated and compared to the EPA's accepted method for particulate measurement. TEOM temperature and flow settings were varied one at a time to evaluate their affect on collection and real-time data. It was found that TEOM temperatures in the 30°C range yielded the best agreement to conventional PM filtration because it is likely that a higher quantity of volatile organic compounds were trapped at this low temperature. However, as sample path temperatures increased, an increase in the positive-to-negative mass ratio was reported. A higher positive-to-negative ratio is useful in real-time PM measurement. A sample path of 50°C gave the highest ratio of positive-to-negative mass ratio. This phenomenon is theorized to be from an increased VOC and moisture rejection rate due to the increase in temperature. A compromise between conventional filter agreement and real-time data was made in selecting the temperature set point of 40°C as the optimum sampling temperature. Sample flow rate was varied from one to four lpm. The conventional filter agreement diverged as TEOM flow increased. The positive-to-negative mass ratio decreased as flow decreased. This trend was theorized to be a reduced resident time for ultrafine PM and volatiles to become attached in the crevices of the filter due to the increased filter face velocity. The flow rate of three lpm was chosen to be a compromise between conventional filtration agreement and real-time characteristics.

The filter collection efficiency of a new filter was found to be a significant source of variability. On average, the first test captured 40% less mass than the third. A two element system would improve this deficiency. The best conventional filtration agreement for an FTP test cycle was a TEOM/conventional ratio of 0.97. The best results for an FTP test set was a three point average TEOM/conventional ratio of 0.92 with a COV percentage of 0.15%. Seven FTP tests taken on two different days with 40°C sample path temperatures and three lpm sample flow rate yielded an average TEOM/conventional ratio of 0.90 and a COV% of 25.62%. When the initial test with a new filter is disregarded, the 99% confidence in TEOM results was ±4.3%. In comparison, the 99% confidence in conventional PM results was 1.7%.

An improvement of only one percent was measured when sample location was moved from the primary dilution tunnel to the secondary dilution tunnel. The real-time data were smoother when sampling from the secondary dilution tunnel when compared to primary dilution tunnel sampling.

The TEOM filter was found to be ready to be used in approximately one minute if it was kept inside the provided storage bag supplied by R&P. If there is a doubt about the filter storage environment, a six minute delay time should be taken to allow the filter to stabilize before a test was started. The current TEOM filter available that yields the best collection efficiency utilizes the TX40

filter media. The TX40 media exhibited better initial collection efficiency and a faster time to asymptote that the T60A20 filter media.

No strong linear correlations were found with HC, CO_2, or NO_x were found. Trends that were observed between TEOM and other emissions were not always constant between test cycles.

8 Recommendations

The TEOM was very sensitive to cycle to cycle variations. The best agreement between TEOM to conventional PM filters for the WVU FTP 75 cycle was 15.1 percent difference (from conventional). This difference could be due to the differing amount of SOF collecting on the two filtering methods. Stabilizing the temperature of the PM sample could reduce deficiencies in the convention method. Currently, the sampling temperature varies with dilution ratio. A SOF content comparison between TEOM and conventional filtration was needed. To improve the TEOM as a real-time filter mass measuring devise, the filter efficiency should be stabilized. A two-stage filter module needs to be developed for use on the TEOM, shown in figure 52. The two-stage filter would be used once, just as the conventional PM filters. A detailed correlation attempt between transient HC, CO and TEOM would be a valuable calibration tool. A method of calculating out the water mass measurement would aid in such a study [19].

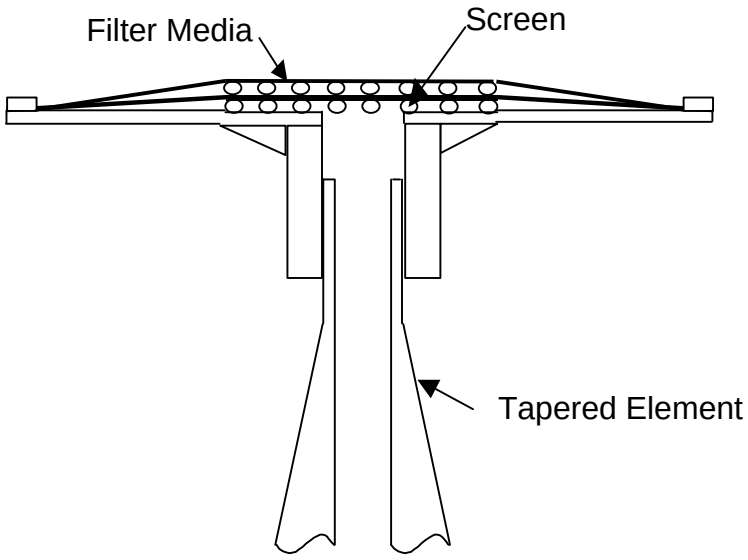

Figure 54: A proposed TEOM filter design.

References

1. HEI Special Report, “Diesel Exhaust: A Critical Analysis of Emissions, Exposure, and Health Effects,” Health Effects Institute, Cambridge, MA, 1995.
2. Environmental Protection Agency, Code of Federal Regulations, Title 40 Part 86 Subpart N, Office of the Federal Register National Archives and Records Administration, July 1, 1998.
3. Ogawa, T., Toshimi, A, Masanori, O., Yoshio, F., “Fuel Effects on Particulate Emissions from D.I. Engine – Chemical Analysis and Characterization of Diesel Fuel,” SAE Paper 95351, 1995.
4. Heywood, J. B., Internal Combustion Engine Fundamentals, McGraw-Hill, New York, NY, 1988.
5. Challen, R., Baraneseu, B., Diesel Engine Reference Book, Second Edition, SAE 1999
6. Kato, S., Takayama, Y., Takeshi, S. G., "Investigation of Particulate Formation of D.I. Diesel Engine with Direct Sampling from Combustion Chamber,” SAE Paper 972969, 1997.
7. Shore, P. R., Cuthberson, R. D., "Application of a Tapered Element Oscillating Microbalance to Continuos Diesel Particulate Measurement,” SAE Paper 850405, 1985.
8. Okrent, D. A., “Optimization of a Third Generation TEOM Monitor for Measuring Diesel Particulate in Real-Time,” SAE Paper 980409, 1998.
9. Whitby, R., Gibbs, R., Johnson, R., Hill, B., Shimpi, S., Jorgeson, R., “Real-Time Diesel Particulate Measurement using a Tapered Element Oscillating Microbalance,” SAE Paper 820463, 1982.
10. Whitby, R., Johnson, R., Gibbs, R., “Second Generation TEOM Filters – Diesel Particulate Mass Comparisons Between TEOM and Conventional Filtration Techniques,” SAE Paper 850403, 1985.
11. Saito, K., Osamu, S., “The Measurement of Diesel Particulate Emissions with a Tapered Element Oscillating Microbalance and an Opacimeter,” SAE Paper 900644, 1990.
12. Sienicki, E., “Status of 1994 Heavy Duty Round Robin Engine Transient Emissions Measurement,” Engine Manufacturing Association Committee Correspondence, Chicago, IL, February 23, 1995.
13. Jarett, R. P., Clark, N. N., “Evaluation of Methods for Determining Continuous Particulate Matter from Transient Testing of Heavy-Duty Diesel Engines,” SAE Paper 2001-01-3575, 2001.
14. Clark, N. N., Gautam, M., Bata, R. M., Wang, W. G., Loth J. L., Palmer, G. M., Lyons, D. W., “Design and Operation of a New Transportable Laboratory for Emissions Testing of Heavy Duty Trucks and Buses,” Int. J. Vehicle Design (Heavy Vehicle Sys.), 1995.
15. Pall-Gelman Sciences Product data, Hydrocarbon, Chemical, Polymer Group, East Hills, NY, April 1998.

16. Clark, N. N., Jarrett, J. P., Atkinson, C. M., “Field Measurements of Particulate Matter Emissions, Carbon Monoxide, and Exhaust Opacity from Heavy-Duty Diesel Vehicles,” ISSN 1047-3289, J. Air and Waste Management Association, Volume 49, pp. 78 - 84, 1999.
17. Beckwith, T. G., Marangoni, R. D., Lienhard, J. H., Mechanical Measurements, Fifth Edition, Addison-Wesley Publishing Company, Inc., Reading, MA, 1993.
18. Messer, J. T., Clark, N.N., Lyons, D.L., "Measurement Delays and Modal Analysis for a Heavy Duty Transportable Emissions Testing Laboratory," SAE Paper 950218, 1995.
19. Jarrett, R. P., Clark, N. N., Gilbert, M., Ramamurthy, R., "Evaluation and Correction of Moisture Adsorption and Desorption from a Tapered Element Oscillating Microbalance," Powder Technology, Volume 119, pp. 215 - 228, 2001.

Appendix A: TEOM configuration files and I/O port pin out

Table 19: The TEOM user configuration, "1105P.CON", file mainly contains data logging information.

Slot		Description	Contents
0	X-Axis	X-Axis Span (min)	30
1		X-Axis Format (code)	0
2	On-Line	Printing Interval (sec)	-300
3	Printing	Mode (0:No 1:Prt 2:Plt)	0
4	On-Line	Disk Drive (A-Z)	D
5	Storage	Subdirectory (name)	teomdata
6		Storage Interval (sec)	0.2
7		Store Data (0:No 1:Yes)	1
8	Y-Axis	Default Left (0-10)	6
9		Default Right (0-10)	7
10	Averaging	TM Calc (0:Ave 1:Exp)	0
11		TM Time Window (sec)	3
12		MR/MC Time Window	3
13	Settings	Sample Flow Rate	2
14		Housing Temperature	40
15		Air Tube Temperature	40
16		Horiba MDT	0
17		Horiba MDT	0
18		External Tube Temp	40
19	Flow Cont	STP Temperature	25
20	Transform	Clip Data (0:No 1:Yes)	0
21		MR Conversion Factor	1
22		MC Conversion Factor	1
23		TM Conversion Factor	1
24	Printing	Contents of Column 01	83
25		Contents of Column 02	84
26		Contents of Column 03	85
27		Contents of Column 04	88
28		Contents of Column 05	89
29		Contents of Column 06	118
30		Contents of Column 07	122
31		Contents of Column 08	177
32	Disk	Contents of Column 01	83
33	Storage	Contents of Column 02	84
34		Contents of Column 03	85
35		Contents of Column 04	123
36		Contents of Column 05	117
37		Contents of Column 06	120
Slot		**Description**	**Contents**

38		Contents of Column 07	122
39		Contents of Column 08	88
40	Analog	Contents	83
41	Output	Chan 1 Minimum Point	-5.00E-07
42		Maximum Point	1.00E-06
43		Contents	84
44		Chan 2 Minimum Point	-4.00E+01
45		Maximum Point	6.00E+01
46		Contents	85
47		Chan 3 Minimum Points	-1.00E-05
48		Maximum Point	2.90E-04
49	Serial Output:	Contents	83
50	Key	Contents | Units	-116 | C
51	Assign	F1 Minimum Point	49.8
52		Step	0.1
53		Contents | Units	-117 | øC
54		F2 Minimum Point	49.8
55		Step	0.1
56		Contents | Units	-118 | øC
57		F3 Minimum Point	49.8
58		Step	0.1
59		Contents | Units	-119 | øC
60		F4 Minimum Point	44.8
61		Step	0.1
62		Contents | Units	83 | g/sec
63		F5 Minimum Point	-2.50E-07
64		Step	2.50E-07
65		Contents | Units	84 | mg/m^3
66		F6 Minimum Point	-4.00E+01
67		Step	2.00E+01
68		Contents | Units	85 | gms
69		F7 Minimum Point	-1.00E-05
70		Step	6.00E-05
71		Contents | Units	88 | Hz
72		F8 Minimum Point	200
73		Step	20
74		Contents | Units	89 | SD
75		F9 Minimum Point	0.00E+00
76		Step	1.00E+06
77		Contents | Units	-122 | in. Hg
78		F10 Minimum Point	0
79		Step	5

Table 20: The instrument configuration file, “1105.INS”, containing critical instrument settings.

Slot		Description	Contents
0	Files	Conversion Files	1105
1		User Config File	1105p
2	Screens	Instrument Title	Series 1105 TEOM Monitor
3		Screen Divisions	5
4	Hardware	Calib Constant (K0)	14166
5		MR/MC/TM Cycle (sec)	0.1048576
6		An/Di Cycle (sec)	0.1048576
7	Country	Language	English
8		Print Code: Compress	15
9		Print Code: Next Page	12
10	Clipping	Time Window (sec)	5
11		In-Clip (0.0-0.5)	0.02
12		Out-Clip (0.0-0.5)	0.02
13	Default	Resistance	51100
14	Temp/Flow	Low Reference	0
15	Constants	High Reference	6
16		T-Constant 1	8.27E-04
17		T-Constant 2	2.09E-04
18		T-Constant 3	8.09E-08
19		Flow Rate Constant	1
20	Counter Board	Board Type	1
21		Base Address	768
22		Board Type	5
23	Analog-In Board	Channels	15
24		Base Address	784
25		Board Type	5
26	Analog-Out Board	Channels	8
27		Base Address	784
28		Board Type	0
29	Digital-In Board	Channels	0
30		Base Address	0
31		Board Type	5
32	Digital-Out Board	Channels	8
33		Base Address	784
34		Readings per Analog Input	12
35		Short Numerical Display	120
36	Numerical Display	01: Row 1L	83
37	Window	02: Row 1M	84
38		03: Row 1R	85
39		04: Row 2L	116
40		05: Row 2M	124
41		06: Row 2R	119
Slot		**Description**	**Contents**

42		07: Row 3L	90
43		08: Row 3M	88
44		09: Row 3R	89
45		10: Row 4L	120
46		11: Row 4M	122
47		12: Row 4R	123
48		13: Row 5L	173
49		14: Row 5M	174
50		15: Row 5R	177
51		16: Row 5L	117
52		17: Row 6M	118
53		18: Row 6R	0
54		19: Row 6L	0
55		20: Row 7M	0
56		21: Row 7R	0
57		22: Row 7L	0
58		23: Row 8M	0
59		24: Row 8R	0
60	AK	Station Number	52
61	Protocol	Channel Number	75048
62		Append Codes	13010
63		Baud Rate	9600
64		Data Bits	8
65		Stop Bits	1
66		Parity	0
67		Handshaking	0
68		Serial Port	2
69	Pres. Comp. (Yes=1/No=0)?		0
70	Bypass(1)/Purge(0) Status		0
71	Warm-Up: Filter Change (sec.)		0
72	Warm-Up: Initial Delay (sec.)		900
73	Collection Data Delay (sec.)		13
74			0
75			0
76			0
78			0
79			0
80			0

Table 21: TEOM channel assignments for the configuration files.

Channel Number	Channel Contents
83	MR
84	MC
85	TM
88	FR
89	SD
90	Xtime
110	UIn1
111	UIn2
112	UIn3
113	UIn4
116	Head
117	Air
118	Cap
119	EST
120	Flow
121	VAC
122	TnlP
123	FltP
124	IST
125	AGCV
137	UO-1
138	UO-2
139	UO-3
173	PCLw
174	PCHi
175	Stat
176	PWM
177	B/PV

Table 22: Pin designations for the user I/O connection for external data collection and remote activation.

Pin/Block Designator	Label
1	User Out 1
2	User Out 2
3	User Out 3
4	Remote Start +
5	User Digital In 1
6	User Digital In 2
7	User Digital In 3
8	User Digital In 4
9	User Out 1 Gnd
10	User Out 2 Gnd
11	User Out 3 Gnd
12	Remote Start Gnd
13	User Digital Gnd
14	User Digital Gnd
15	User Digital Gnd

Table 23: TTL control logic for remote collection.

User Digital In 1	User Digital In 2	Operation Mode Selected
<2.5 volts	<2.5 volts	No Change
>=2.5 volts	<2.5 volts	Collection
<2.5 volts	>=2.5 volts	Stop
>=2.5 volts	>=2.5 volts	Initialization

Appendix B: Time Shifting Program

```
Sub crosscorrmyway()
'
' CrossCorro Macro
' Cross Corrolation Macro
'
' Keyboard Shortcut: Ctrl+Shift+C
'
'This program uses the excel function CORREL to determine the time shift of
'continuous emission data readings with that of the engine (or axial) torque to
'provide maximum correlation.  The program was designed to read from an Excel
'spread sheet. The program uses the first column (Time)to calculate the number
'of data points and the sample rate. The next column should be power (engine or
'axial), hub speed, or engine speed. The nest column should be the first emission
'column.  There should also be 2 rows at the top as header (first row being
'emission, second row being unit).

Dim Rmax(7), t(7), NewR(1000, 7), OldR As Single
Dim A As Range, B As Range
Dim label(7) As String
Dim sps As Integer

I = 0
Sum = 0
x = 0
'Time Range for evaluation in seconds
tr = 40

'Find the range of the data
Range("a3").Select
Do While ActiveCell.Offset(x, 0) > ""
x = x + 1
```

```
Loop

'find samples per second (sps)
sps = 1 / (ActiveCell.Offset(x - 19, 0) - ActiveCell.Offset(x - 20, 0))
tr = tr * sps

'find number of labels
y = 0
Range("b1").Select
Do While ActiveCell.Offset(0, y + 1) > ""
   label(y + 1) = ActiveCell.Offset(0, y + 1)
   y = y + 1
Loop


'This cell was the start of the power or speed data
Range("b2").Select

For z = 1 To y 'z = the number of emission columns

   timeshift = 1
   NewR(timeshift, z) = 0
   Rmax(z) = 0

   For timeshift = 1 To tr
      Set A = Range(ActiveCell.Offset(1, 0), ActiveCell.Offset((x - timeshift), 0))
      Set B = Range(ActiveCell.Offset(1 + timeshift, z), ActiveCell.Offset(x, z))
      NewR(timeshift, z) = Application.WorksheetFunction.Correl(A, B)

      'finding max correlation
      If NewR(timeshift, z) > Rmax(z) Then
         Rmax(z) = NewR(timeshift, z)
         t(z) = timeshift
        'OldR = NewR(timeshift, z)
```

```
        'else if NewR(timeshift, z) < Rmax(z)then

        End If


    Next timeshift

Next z

'Print out
Sheets.Add.Name = "cross correlation"
Range("a1").Select
ActiveCell.Offset(0, 1) = "Time Shift"
ActiveCell.Offset(0, 2) = "Emission"
ActiveCell.Offset(1, 1) = "(seconds)"
ActiveCell.Offset(2, 0) = "time @ best correl"
ActiveCell.Offset(3, 0) = "best correl"


For z = 1 To y
    ActiveCell.Offset(1, z + 1) = label(z)
    ActiveCell.Offset(2, z + 1) = t(z) / sps
    ActiveCell.Offset(3, z + 1) = Rmax(z)
    For timeshift = 1 To tr
        ActiveCell.Offset(timeshift + 3, 1) = timeshift / sps
        ActiveCell.Offset(timeshift + 3, z + 1) = NewR(timeshift, z)
    Next timeshift
Next z
End Sub
```

Appendix C: Verification of the Time Shifting Program

The output of the time shifting program was figure 35 and table 24. The program indicated that the shifts necessary for CO and CO_2 power correlation were greater than 20 seconds. It is stated in the CFR [2] that the maximum response time of the analyzers must be less than 20 seconds of the step change. To verify the programs suggested time shift: (1) the emission traces were plotted with power to verify correlation and (2) the data shift was verified by using the coefficient of determination (r^2) to find the best shift.

Table 24: The time shifts for CO and CO_2 emissions suggested by the correlation program exceeded the EPA recommended 20 second maximum.

Emission	HC	CO	CO_2	NO_x	TEOM
Suggested Shift (sec)	19.2	22.6	22.4	11.2	5.2

The gaseous emissions were plotted with power on the time scale to verify correlation between emissions and engine power. Correlation was considered present if a change in gaseous emissions followed a change in power. The strength of the correlation is not of concern here. A small excerpt of the FTP data that was discussed in chapter 6 is illustrated in figure 55. The gaseous emissions graphed are time shifted per the recommendations of the shifting program in Appendix B. In the figure, power increased after a long idle as did emissions and generally, emission subsided when power decreased. However, it can be seen that the emissions are shifted in advance of the first power rise. This is thought to be unrealistic because the ideal engine does not increase pollutants in anticipation of a transient. The recommended visual shift based on initialization is listed in table 25. Unfortunately, CO and CO_2 emissions were still greater than 20 seconds. The cause of the long time shifts was unknown.

Table 25: The recommended emission shifts base on the alignment of emission and power increase after an idle. Unfortunately, these time shifts also exceed the 20 second EPA guidelines.

Emission	HC	CO	CO_2	NO_x	TEOM
Suggested Shift (sec)	14.4	21.4	20.2	10.0	3.2

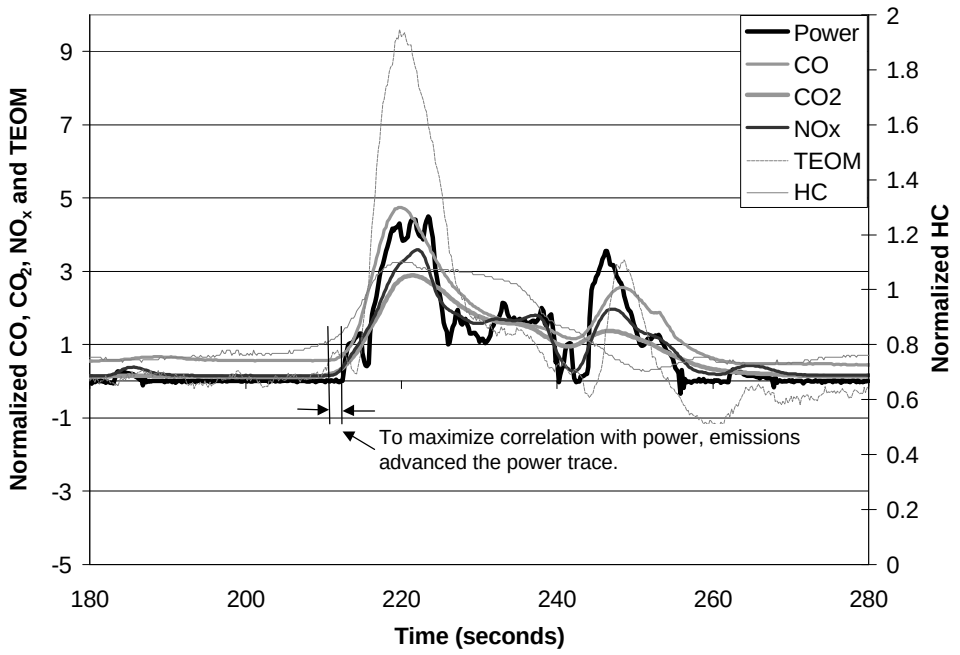

Figure 55: A section of real-time FTP data shifted per the program's recommended amount. It can be seen here that the compromise to best power correlation is an unrealistic advance of the emission data.

To verify the correlation of the time shift program, another method of correlation was applied to the NO_x and CO_2 data sets. The emissions data were shifted forward with respect to engine power, which remained stationary. As the data were shifted, the coefficient of determination (r^2) was recorded. The best time shift was declared when the r^2 value reached a maximum. This is represented graphically in figure 56. The maximum correlation occurred at 11.2 seconds for the NO_x data and 22.4 seconds for the CO_2 data. This result matched the program's recommended shift.

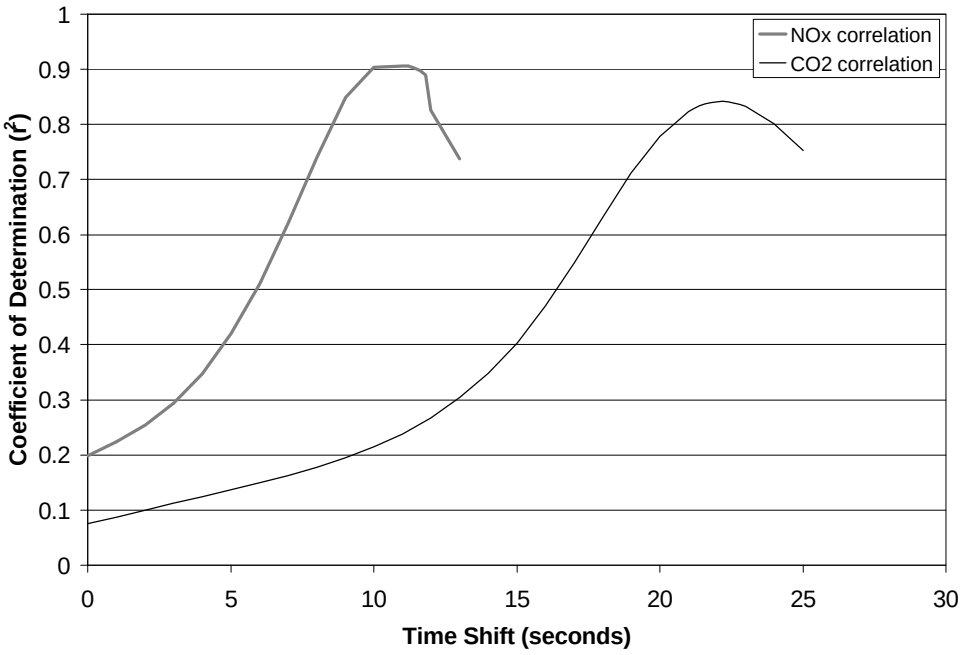

Figure 56: Results from cross correlating engine power with NO_x and CO_2 using the coefficient of determination. The time at peak correlation using this method is equal to the time shift of the program.